

JAERI - M
82-188

FULL-SCALE MARK II CRT PROGRAM : DYNAMIC RESPONSE
EVALUATION TEST OF PRESSURE TRANSDUCERS

December 1982

Yutaka KUKITA, Ken NAMATAME, Isao TAKESHITA
and Masayoshi SHIBA

JAERI-Mレポートは、日本原子力研究所が不定期に公刊している研究報告書です。
入手の問合わせは、日本原子力研究所技術情報部情報資料課（〒319-11茨城県那珂郡東海村）あて、お申しこしてください。なお、このほかに財団法人原子力弘済会資料センター（〒319-11 茨城県那珂郡東海村日本原子力研究所内）で複写による実費頒布をおこなっております。

JAERI-M reports are issued irregularly.

Inquiries about availability of the reports should be addressed to Information Section, Division of Technical Information, Japan Atomic Energy Research Institute, Tokai-mura, Naka-gun, Ibaraki-ken 319-11, Japan.

©Japan Atomic Energy Research Institute, 1982

編集兼発行 日本原子力研究所
印刷 いばらき印刷株式会社

Full-Scale Mark II CRT Program : Dynamic Response
Evaluation Test of Pressure Transducers

Yutaka KUKITA, Ken NAMATAME, Isao TAKESHITA
and Masayoshi SHIBA

Division of Nuclear Safety Research,
Tokai Research Establishment, JAERI

(Received November 17, 1982)

A dynamic response evaluation test of pressure transducers was conducted in support of the JAERI Full-Scale Mark II CRT (Containment Response Test) Program. The test results indicated that certain of the cavity-type transducers used in the early blowdown test had undesirable response characteristics. The transducer mounting scheme was modified to avoid trapping of air bubbles in the pressure transmission tubing attached to the transducers. The dynamic response of the modified transducers was acceptable within the frequency range of 200 Hz.

Keywords: Pressure Transducer, Dynamic Response, Mark II Containment, Hydrodynamic Loads, Reactor Safety

This work was performed under the auspices of the Japan Science and Technology Agency.

This report supercedes JAERI internal document JAERI-memo 9847 (Dec. 1981).

格納容器圧力抑制系信頼性実証試験

圧力変換器の動特性試験

日本原子力研究所東海研究所安全工学部

久木田 豊・生田目 健・竹下 功・斯波 正誼

(1982年11月17日受理)

格納容器圧力抑制系信頼性実証試験に使用されている圧力変換器の動特性を、既知の特性を有する変換器との比較によって計測した。この結果、良好な特性を得るためには導圧管内の気泡の除去に注意すべきことが明らかになった。本試験結果にもとづき圧力変換器の改造を行い、200 Hz以下の周波数で十分に良好な特性が得られるようになった。また、導圧管の共振周波数が集中定数系モデルにより予測できることを示した。

この報告書は、電源開発促進対策特別会計施行令にもとづき、科学技術庁から日本原子力研究所への委託研究：昭和55年度「格納容器圧力抑制系信頼性実証試験」のうち、圧力変換器の動特性に関する試験結果をまとめたものである。

本報告は、先に作成した原研所内資料 JAERI-memo 9847 (1981年12月)の内容に検討・修正を加え、公開に付するものである。

CONTENTS

1. Introduction	1
2. Transducer design and mounting schemes	2
3. Test apparatus and test procedure	2
4. Data reduction procedure	4
5. Test results	6
6. Modified transducer designs	7
7. Conclusions	8
Acknowledgements	9
References	9
Appendix A Analysis of air bubble effects on transducer response	45
Appendix B Acceleration sensitivity of pressure transducer	48
Appendix C Further improvements on pressure measurement	56

目 次

1. まえがき	1
2. 圧力変換器の構造および取付け方法	2
3. 試験装置および試験方法	2
4. データ処理方法	4
5. 試験結果	5
6. 圧力変換器の改造	7
7. 結 論	8
謝 辞	9
参考文献	9
付 録	45
A. 導圧管内の空気泡の影響に関する解析	45
B. 圧力変換器に対する加速度の影響	48
C. ブローダウン試験中の圧力変換器動特性	56

List of Tables and Figures

Table 1	Specifications of tested pressure transducer
Table 2	Physical properties of silicon oil
Table 3	Specifications of signal conditioner
Table 4	Specifications of reference pressure transducer
Table 5	Specifications of charge amplifier, Kistler
Table 6	Specifications of accelerometer
Table 7	Specifications of charge amplifier, Bruel & Kjaer
Table 8	Specifications of DC amplifier, Toyoda
Table 9	Specifications of DC amplifier, Kyowa
Table 10	Test matrix, original transducers
Table 11	Test matrix, modified transducer
Fig. 1	Cross-section of cavity-type pressure transducer
Fig. 2	Pressure transducer installation scheme: wall pressure transducer
Fig. 3	Pressure transducer installation scheme: bottom pressure transducer
Fig. 4	Schematic of test apparatus
Fig. 5	Block diagram of test equipment
Fig. 6	Test arrangement for bottom transducer
Fig. 7	Test arrangement for wall transducer
Fig. 8	Gain and phase characteristics of built-in low-pass-filter of Kyowa signal conditioner
Fig. 9	Block diagram of data-processing computer program
Fig. 10	Gain response of wall transducer, 350 kPa system pressure
Fig. 11	Phase response of wall transducer, 350 kPa system pressure
Fig. 12	Gain response of wall transducer, 250 kPa system pressure
Fig. 13	Phase response of wall transducer, 250 kPa system pressure
Fig. 14	Gain response of wall transducer, 150 kPa system pressure
Fig. 15	Phase response of wall transducer, 150 kPa system pressure
Fig. 16	Gain response of bottom transducer, 350 kPa system pressure
Fig. 17	Phase response of bottom transducer, 350 kPa system pressure
Fig. 18	Gain response of bottom transducer, 250 kPa system pressure
Fig. 19	Phase response of bottom transducer, 250 kPa system pressure
Fig. 20	Gain response of bottom transducer, 150 kPa system pressure
Fig. 21	Phase response of bottom transducer, 150 kPa system pressure

- Fig. 22 Gain response of bottom transducer, 350 kPa system pressure
"air-free" test
- Fig. 23 Phase response of bottom transducer, 350 kPa system pressure
"air-free" test
- Fig. 24 Modified mounting scheme for bottom transducer
- Fig. 25 Pressure tubing inlet designs
- Fig. 26 Gain response of modified transducer, 350 kPa system pressure
- Fig. 27 Phase response of modified transducer, 350 kPa system pressure
- Fig. 28 Gain response of modified transducer, 250 kPa system pressure
- Fig. 29 Phase response of modified transducer, 250 kPa system pressure
- Fig. 30 Gain response of modified transducer, 150 kPa system pressure
- Fig. 31 Phase response of modified transducer, 150 kPa system pressure
- Fig. 32 Modified mounting scheme for vent pipe transducer
- Fig. 33 Significance of system vibration effects during tests of
modified transducer
- Fig. A-1 Modeling of pressure transmission tubing containing air bubble
- Fig. A-2 Comparison of measured and calculated natural frequencies of
pressure transmission tubing containing air bubble
- Fig. B-1 Mounting scheme of Entran flush-diaphragm transducer
- Fig. B-2 Comparison of output signals from flush-diaphragm and cavity-
type transducers
- Fig. B-3 Setup of acceleration sensitivity test
- Fig. B-4 Acceleration sensitivity of pressure transducer without
silicon oil
- Fig. B-5 Acceleration sensitivity of pressure transducer with silicon
oil filled in pressure transmission tubing
- Fig. B-6 Modeling of transducer response to acceleration
- Fig. C-1 Dynamic response of cavity-type transducer evaluated using
Entran transducer as reference
- Fig. C-2 Dynamic response of cavity-type transducer evaluated using
Senso-Metrics transducer as reference

1. Introduction

This report documents a dynamic response evaluation test of the cavity-type pressure transducers used in the JAERI Full-Scale Mark II CRT (Containment Response Test).

The CRT Program was initiated in 1977 to provide a data base for the licensing evaluation of the hydrodynamic loads induced in the BWR Mark II pressure suppression containment system during a hypothetical LOCA (loss of coolant accident).

Among the specific test objectives of the CRT was to define the magnitudes of the pressure loads acting on the pressure suppression pool boundaries. For that purpose, many pressure transducers were installed on the pool bottom and wall. To conduct reliable measurement, transducers were required to have appropriate dynamic as well as static response characteristics. Considering the energy spectra of the pressure loads to be measured in the CRT facility, a flat frequency response up to 200 Hz was thought to be desirable.

A cavity-type transducer design was selected for use in the CRT facility¹⁾. Although the transducers proved to have satisfactory static response characteristics adequacy of their dynamic response characteristics was questioned through observation of the test data from the early test runs. For example, the pool bottom transducers indicated inconsistently higher amplitudes of the pressure oscillations than the low-elevation (1.8 m) wall transducers did (e.g., see Plots S-12 to S-23 of Reference 2). Due to this concern a special test was designed to evaluate the dynamic response of the pressure transducers used for measurement of the pool boundary pressures. The test was initiated in April 1980 and indicated an undesirable dynamic response of the pool bottom transducer.

An alternative transducer mounting scheme in combination with a new tubing inlet design, the transducer dynamic response with which was confirmed by tests to be acceptable, was adopted for the pool boundary transducers including those on the wall, and has been used from TEST 3103 conducted on September 19, 1980.

Some indications of deficiency were observed also for the vent pipe pressure transducers, though to date any systematic evaluation has not been conducted for them. Accordingly, modification was made also for the vent pipe transducers along with the modification of the pool boundary transducers.

The evaluation test results are compared with a simplified mass-spring-system analysis in Appendix A.

In addition, the acceleration sensitivity of the cavity-type pressure transducer was evaluated and is compared with an analysis in Appendix B.

2. Transducer design and mounting schemes¹⁾

The cross-sectional view and design specifications of the cavity-type pressure transducers are presented in Fig. 1 and Table 1. To avoid the temperature effects each transducer is installed in a water-jacketed housing. A pressure tubing (10 mm I.D.) penetrates the housing. The tubing and the transducer cavity (ca. 11700 mm³) is filled with high-viscosity silicon oil, whose physical properties are listed in Table 2.

All the transducers are installed on the pool boundaries from the inside, i.e., the transducers are submerged in the pool water. The mounting scheme depends on the location of the measuring point as shown in Figs. 2 and 3. The bottom transducers were mounted with their axes parallel to the horizontal bottom floor, while the wall transducers were mounted with their axes parallel to the vertical wall.

3. Test apparatus and test procedure

A special test apparatus shown in Fig. 4 was designed for the present evaluation test. The block diagram of the apparatus is shown in Fig. 5 and specifications of the equipments are listed in Tables 3 through 9. The test apparatus consists of a test vessel, an electromagnetic shaker, transducers with signal electronics, and a data acquisition system. The test vessel is a stainless-steel thick-walled cylindrical vessel mounted on a concrete base mat, and has a flexible diaphragm on one of its ends and a test section on the other. The test vessel is filled with water of room temperature. The system pressure is raised by a manual pump up to values representing the containment static pressure during the actual blowdown experiments. Harmonic pressure oscillations are generated in the water by exciting the diaphragm by the electromagnetic shaker. A wave generator supplies sinusoidal wave signal to a power amplifier which drives the shaker. The signal frequency is varied manually.

The evaluation test results are compared with a simplified mass-spring-system analysis in Appendix A.

In addition, the acceleration sensitivity of the cavity-type pressure transducer was evaluated and is compared with an analysis in Appendix B.

2. Transducer design and mounting schemes¹⁾

The cross-sectional view and design specifications of the cavity-type pressure transducers are presented in Fig. 1 and Table 1. To avoid the temperature effects each transducer is installed in a water-jacketed housing. A pressure tubing (10 mm I.D.) penetrates the housing. The tubing and the transducer cavity (ca. 11700 mm³) is filled with high-viscosity silicon oil, whose physical properties are listed in Table 2.

All the transducers are installed on the pool boundaries from the inside, i.e., the transducers are submerged in the pool water. The mounting scheme depends on the location of the measuring point as shown in Figs. 2 and 3. The bottom transducers were mounted with their axes parallel to the horizontal bottom floor, while the wall transducers were mounted with their axes parallel to the vertical wall.

3. Test apparatus and test procedure

A special test apparatus shown in Fig. 4 was designed for the present evaluation test. The block diagram of the apparatus is shown in Fig. 5 and specifications of the equipments are listed in Tables 3 through 9. The test apparatus consists of a test vessel, an electromagnetic shaker, transducers with signal electronics, and a data acquisition system. The test vessel is a stainless-steel thick-walled cylindrical vessel mounted on a concrete base mat, and has a flexible diaphragm on one of its ends and a test section on the other. The test vessel is filled with water of room temperature. The system pressure is raised by a manual pump up to values representing the containment static pressure during the actual blowdown experiments. Harmonic pressure oscillations are generated in the water by exciting the diaphragm by the electromagnetic shaker. A wave generator supplies sinusoidal wave signal to a power amplifier which drives the shaker. The signal frequency is varied manually.

The evaluation test results are compared with a simplified mass-spring-system analysis in Appendix A.

In addition, the acceleration sensitivity of the cavity-type pressure transducer was evaluated and is compared with an analysis in Appendix B.

2. Transducer design and mounting schemes¹⁾

The cross-sectional view and design specifications of the cavity-type pressure transducers are presented in Fig. 1 and Table 1. To avoid the temperature effects each transducer is installed in a water-jacketed housing. A pressure tubing (10 mm I.D.) penetrates the housing. The tubing and the transducer cavity (ca. 11700 mm³) is filled with high-viscosity silicon oil, whose physical properties are listed in Table 2.

All the transducers are installed on the pool boundaries from the inside, i.e., the transducers are submerged in the pool water. The mounting scheme depends on the location of the measuring point as shown in Figs. 2 and 3. The bottom transducers were mounted with their axes parallel to the horizontal bottom floor, while the wall transducers were mounted with their axes parallel to the vertical wall.

3. Test apparatus and test procedure

A special test apparatus shown in Fig. 4 was designed for the present evaluation test. The block diagram of the apparatus is shown in Fig. 5 and specifications of the equipments are listed in Tables 3 through 9. The test apparatus consists of a test vessel, an electromagnetic shaker, transducers with signal electronics, and a data acquisition system. The test vessel is a stainless-steel thick-walled cylindrical vessel mounted on a concrete base mat, and has a flexible diaphragm on one of its ends and a test section on the other. The test vessel is filled with water of room temperature. The system pressure is raised by a manual pump up to values representing the containment static pressure during the actual blowdown experiments. Harmonic pressure oscillations are generated in the water by exciting the diaphragm by the electromagnetic shaker. A wave generator supplies sinusoidal wave signal to a power amplifier which drives the shaker. The signal frequency is varied manually.

The dynamic response of the cavity-type transducer was evaluated using a reference transducer. A Kistler Type 7261 piezoelectric flush-diaphragm transducer was used as the reference. Since the Kistler transducer is guaranteed for a frequency range of 13 kHz, it provides a reliable reference for the tested frequency range of 10 to 228 Hz. The reference and the test transducers were mounted on the test section to be close to each other to ensure that the differences in magnitude and phase of the pressures acting on the two transducers be negligibly small. The test arrangements for the bottom and the wall transducers are shown in Figs. 6 and 7. To ease mounting of the transducer on the test section the water jacket was removed from the assembly, however, the configuration of the pressure tubing was preserved. Thus, by comparison of the output signals from the reference and the test transducers, the gain and phase responses of the tested transducer was evaluated.

The amplitudes of the obtained pressure oscillations in the test vessel was generally small (typically 1 kPa_{p-p}), so that a high dynamic sensitivity was required for the measurement. The output signals from the two pressure transducers were high-pass-filtered at a cut-off frequency of 3 Hz to reject D.C. offset, and amplified from 20 to 50 times.

The present evaluation test was conducted with use of the same type of signal conditioner as used in the blowdown experiments with the LPF activated. It was found by tests, however, that the LPF induces considerable phase shifts even below its nominal cut-off frequency as shown in Fig. 8. Namely, the obtained test results (Figs. 10 to 31) include the gain and phase deviations caused by the LPF.

During the preliminary test runs on this test apparatus, the obtained frequency response curves indicated several peaks and dips difficult to interpret. Careful study of the data revealed that vibration of the system affected the output signal from the tested cavity-type transducer. Namely, vibration of the test section caused acceleration of the silicon oil leg contained in the pressure tubing and resulted in "acoustic equivalent" signal, whereas the reference Kistler transducer being rather insensitive to acceleration. Finally, a mass of concrete was cast outside the test vessel to increase the mass and stiffness of the test system. Thus the system vibration was significantly reduced, however, it was still present and had some effects on the data especially at the higher frequencies where the obtained pressure amplitude were generally small. To monitor the vibration of the test section a Bruel of Kjaer

Type 4370 accelerometer was installed as shown in Fig. 4.

Before casting concrete around the test vessel, a "dry test" was conducted. The test was done without filling water in the vessel, the transducer output signal which was completely "acoustic equivalent", was recorded together with the accelerometer output. Thus evaluated acceleration sensitivity of the tested transducer was used for interpretation of the test data to check the effects of the system vibration on the data. After completion of the present dynamic pressure testing, a more systematic acceleration sensitivity test of was performed with assistance of the transducer vendor. The test results are presented in Appendix B of this report.

4. Data reduction procedure

The output signals from the wave generator, the reference and the tested pressure transducers, and the accelerometer were recorded by an EMR PCM data acquisition system which is used also for the data recording during the blowdown experiment. The data was sampled at 455.56 Hz/channel. Therefore, the Nyquist frequency was 227.78 Hz. The data was transferred to an OKITAC-50 mini-computer and stored in magnetic tapes. The tapes were processed by a FACOM 230-75 computer system of the JAERI computing center.

Although the electromagnetic shaker was driven by a sinusoidal signal, the measured pressure included higher harmonics and noise. Therefore a filtering process was necessary to evaluate the gain and phase characteristics of the transducer. A computer program was developed, whose flow diagram is shown in Fig. 9. First, the data was divided into mutually overlapping time blocks so that each block contains 1024 data points. Then every block of the data was processed by an FFT (fast Fourier transform) subroutine. The dominant frequency is tracked by finding the peak absolute value of the Fourier transform of the wave generator signal. Using the Fourier transforms X and Y of the signals x and y from the reference and the tested transducers respectively, power spectral density (PSD) functions S_x and S_y , and cross power spectral density (CPSD) function S_{xy} were obtained as (to within a constant):

Type 4370 accelerometer was installed as shown in Fig. 4.

Before casting concrete around the test vessel, a "dry test" was conducted. The test was done without filling water in the vessel, the transducer output signal which was completely "acoustic equivalent", was recorded together with the accelerometer output. Thus evaluated acceleration sensitivity of the tested transducer was used for interpretation of the test data to check the effects of the system vibration on the data. After completion of the present dynamic pressure testing, a more systematic acceleration sensitivity test of was performed with assistance of the transducer vendor. The test results are presented in Appendix B of this report.

4. Data reduction procedure

The output signals from the wave generator, the reference and the tested pressure transducers, and the accelerometer were recorded by an EMR PCM data acquisition system which is used also for the data recording during the blowdown experiment. The data was sampled at 455.56 Hz/channel. Therefore, the Nyquist frequency was 227.78 Hz. The data was transferred to an OKITAC-50 mini-computer and stored in magnetic tapes. The tapes were processed by a FACOM 230-75 computer system of the JAERI computing center.

Although the electromagnetic shaker was driven by a sinusoidal signal, the measured pressure included higher harmonics and noise. Therefore a filtering process was necessary to evaluate the gain and phase characteristics of the transducer. A computer program was developed, whose flow diagram is shown in Fig. 9. First, the data was divided into mutually overlapping time blocks so that each block contains 1024 data points. Then every block of the data was processed by an FFT (fast Fourier transform) subroutine. The dominant frequency is tracked by finding the peak absolute value of the Fourier transform of the wave generator signal. Using the Fourier transforms X and Y of the signals x and y from the reference and the tested transducers respectively, power spectral density (PSD) functions S_x and S_y , and cross power spectral density (CPSD) function S_{xy} were obtained as (to within a constant):

$$S_x = X^*X, \quad S_y = Y^*Y \quad (1)$$

$$S_{xy} = X^*Y \quad (2)$$

where an asterisk denotes a complex conjugate. The gain and phase functions of the tested transducers are calculated for the dominant frequency. The gain function, which is the gain of the tested transducer relative to the reference transducer, is defined as:

$$G = \sqrt{S_y/S_x} \quad (3)$$

and the relative phase lag is defined as:

$$\phi = \text{Arg}(S_{xy}) \quad (4)$$

i.e., a positive phase angle indicates a negative phase lag. More strictly the gain and phase functions should be defined as:

$$G' = \overline{S_{xy}}/\overline{S_x} \quad (5)$$

$$\phi' = \text{Arg}(\overline{S_{xy}}) \quad (6)$$

where an overscore denotes averaging over time intervals, to reduce effects of the incoherent noise components contained in the signal y . However, effects of the noise on G and ϕ may be negligibly small unless the amplitude of pressure is excessively small. Actually, the response curves calculated by the equations (3) and (4) indicated small and allowable discrepancies caused by the noise and computation errors.

5. Test results

Tests were conducted for the bottom and the wall transducers at three values of the system pressures (150, 250 and 350 kPa) as summarized in Table 10. It should be noted that in the blowdown experiments adequate dynamic responses of the transducers are especially desired for the measurement of the chugging pressure oscillation which contains high frequency components. The chugging oscillation occurs in the later phase of the blowdown, when the static pressure on the pool boundaries is in the range of 300 to 350 kPa.

$$S_x = X^*X, \quad S_y = Y^*Y \quad (1)$$

$$S_{xy} = X^*Y \quad (2)$$

where an asterisk denotes a complex conjugate. The gain and phase functions of the tested transducers are calculated for the dominant frequency. The gain function, which is the gain of the tested transducer relative to the reference transducer, is defined as:

$$G = \sqrt{S_y/S_x} \quad (3)$$

and the relative phase lag is defined as:

$$\phi = \text{Arg}(S_{xy}) \quad (4)$$

i.e., a positive phase angle indicates a negative phase lag. More strictly the gain and phase functions should be defined as:

$$G' = \overline{S_{xy}}/\overline{S_x} \quad (5)$$

$$\phi' = \text{Arg}(\overline{S_{xy}}) \quad (6)$$

where an overscore denotes averaging over time intervals, to reduce effects of the incoherent noise components contained in the signal y . However, effects of the noise on G and ϕ may be negligibly small unless the amplitude of pressure is excessively small. Actually, the response curves calculated by the equations (3) and (4) indicated small and allowable discrepancies caused by the noise and computation errors.

5. Test results

Tests were conducted for the bottom and the wall transducers at three values of the system pressures (150, 250 and 350 kPa) as summarized in Table 10. It should be noted that in the blowdown experiments adequate dynamic responses of the transducers are especially desired for the measurement of the chugging pressure oscillation which contains high frequency components. The chugging oscillation occurs in the later phase of the blowdown, when the static pressure on the pool boundaries is in the range of 300 to 350 kPa.

The wall pressure transducer indicated acceptable dynamic responses as shown in Figs. 10 to 15. The measured gain and phase lag increased with frequency. For the system pressure of 350 kPa gain increase was 0.5 dB (6%) at 100 Hz and 2 dB (25%) at 200 Hz. The phase lag was 30° at 100 Hz and 70° at 200 Hz. The phase lag mainly came from the builtin LPF of the signal conditioner (Fig. 8). The system pressure had slight effects on the gain and phase responses.

Preliminary test results for the bottom transducer indicated that air bubbles were very likely trapped in the horizontal pressure tubing and in the transducer cavity if not carefully removed. The air bubble effect on the dynamic response might depend on the amount and spatial distribution of air in the tubing. Though the objective of the present tests was to evaluate the transducer dynamic response during the actual blowdown experiments, the amount and distribution of air for the individual transducer during the individual test was not known. Therefore, what was done was to conduct the tests by preparing the transducer in the same manner as for the actual blowdown experiments. Namely, the transducer was held horizontally and silicon oil was injected from the tubing inlet.

Thus prepared bottom pressure transducer indicated undesirable dynamic responses. As shown in Figs. 16 to 21, a single and broad resonance peak was observed in every gain response. Both of the resonance frequency and the peak gain increased with the system pressure: 5 dB at 30 Hz for the 150 kPa system pressure, 8 dB at 49 Hz for 250 kPa, and 9.5 dB at 68 Hz for 350 kPa. Approximate repeatability of the test results was confirmed. It is very clear that the presence of the trapped air, especially in the cavity in front of the transducer diaphragm, lowered the natural frequency of the pressure transmission tubing. The dependency of the dynamic response on the system pressure is due to variation of air compressibility with pressure.

An additional test (PT9274) was conducted on the bottom pressure for the "air free" condition: after filling silicon oil the transducer assembly was held upright till the air bubbles were vented. The test results for this case (Figs. 22 and 23), in comparison with other results, indicated that the transducer itself has an acceptable response if air bubbles are carefully removed.

6. Modified transducer designs

From the results of the present tests, necessity of modification of the bottom transducer design was recognized. The deficiency being caused by the trapped air, modification of the transducer mounting scheme to one which allows natural venting of air bubbles seemed to be a reasonable resolution of the problem. The modified design for the bottom transducer is shown in Fig. 24. In the new design the transducer is mounted vertically. In addition, the pressure transmission tubing is replaced by a straight and shorter one. Also the inlet of the tubing is modified to reduce the possible dynamic flow losses at the inlet ports as shown in Fig. 25.

The test matrix and the test results for the modified transducer is shown in Table 11 and Figs. 26 through 31 respectively. The dynamic response of the modified transducer appears acceptable at least up to 150 Hz, and is even better than that of the wall transducer (Fig. 10 to 15), which means that the configuration of the tubing inlet port had some effect on the response.

As shown in Figs. 26 to 31, the evaluated dynamic response of the modified transducer exhibited dependency on the system pressure. The dynamic response was slightly worse for the lower system pressure. Similar tendency was observed for the wall transducer before the modification (Figs. 10 to 15). These results are uneasy to interpret since these transducers are free from the air effects. Examination of the test results revealed that the system vibration had non-negligible effects on the evaluated response as has been suggested previously. In Fig. 33 the ratios between the system acceleration and the pressure (measured by the Kistler transducer) for the tests on the modified transducer are plotted in an arbitrary unit. The ratio was greater for the lower system pressure. This result might be interpreted that at the lower system pressures the rubber diaphragm of the test apparatus is so flexible that the driving force at the diaphragm cannot efficiently generate pressure variation in the test vessel while it generates the system vibration. Also, the ratio increases with frequency, i.e., acceleration effects on the transducer became more significant at the higher frequencies. The deviation of the dynamic response from the best one (350 kPa system pressure) seems to appear when the ratio exceeds a critical value around 0.01 to 0.05. Finally, it was concluded that the modified transducer

has a flat response within 0.5 dB up to 200 Hz independently from the system pressure, and the wall transducer before modification had a flat response within 2 dB up to 200 Hz. This conclusion was supported by the results of the acceleration sensitivity test described in Appendix B.

Consequently, the new transducer design with improved dynamic response was adopted for all the pool boundary (bottom and wall) transducers. The modification was made in July 1980, between TESTs 3201 and 3103. At the same time the mounting scheme of the vent pipe transducers was altered. In the original design the transducers were connected to the vent pipes with 300 mm to 500 mm long pressure tubings (see Figs. 7.14 and 7.15 of Reference 1). The tubings are partially filled with gas phase (steam) and partially with liquid (silicon oil and water) during the blowdown experiments. Therefore, their transmission characteristics were uncertain. In the new design the transducer is connected to the vent pipe with a short and slanted tubing (Fig. 31). Though test has not been conducted for the old and new vent pipe transducer designs, the dynamic response of the new transducer is thought to be the same or better than that of the new pool boundary transducer.

7. Conclusions

- 1) Dynamic response of the cavity-type pressure transducers used in the CRT facility was evaluated by imposing harmonic pressure variation on the transducers.
- 2) The transducers with horizontal pressure transmission tubings, which were used for measurement of the pool bottom pressure till TEST 3201, proved to be deficient with undesirable air bubble effects on the dynamic response at frequencies higher than 30 Hz. Whereas other transducers, with vertical tubings, indicated acceptable dynamic responses.
- 3) A modified transducer mounting scheme, which allows natural venting of air bubbles, with a shortened tubing was tested. The evaluated dynamic response was satisfactory up to 200 Hz.
- 4) All the pool boundary (bottom and wall) transducers were modified. Also the pressure tubings of the vent pipe transducers were shortened. The modification was completed before TEST 3103.
- 5) The tests indicated that the cavity-type transducer is fairly sensitive

has a flat response within 0.5 dB up to 200 Hz independently from the system pressure, and the wall transducer before modification had a flat response within 2 dB up to 200 Hz. This conclusion was supported by the results of the acceleration sensitivity test described in Appendix B.

Consequently, the new transducer design with improved dynamic response was adopted for all the pool boundary (bottom and wall) transducers. The modification was made in July 1980, between TESTs 3201 and 3103. At the same time the mounting scheme of the vent pipe transducers was altered. In the original design the transducers were connected to the vent pipes with 300 mm to 500 mm long pressure tubings (see Figs. 7.14 and 7.15 of Reference 1). The tubings are partially filled with gas phase (steam) and partially with liquid (silicon oil and water) during the blowdown experiments. Therefore, their transmission characteristics were uncertain. In the new design the transducer is connected to the vent pipe with a short and slanted tubing (Fig. 31). Though test has not been conducted for the old and new vent pipe transducer designs, the dynamic response of the new transducer is thought to be the same or better than that of the new pool boundary transducer.

7. Conclusions

- 1) Dynamic response of the cavity-type pressure transducers used in the CRT facility was evaluated by imposing harmonic pressure variation on the transducers.
- 2) The transducers with horizontal pressure transmission tubings, which were used for measurement of the pool bottom pressure till TEST 3201, proved to be deficient with undesirable air bubble effects on the dynamic response at frequencies higher than 30 Hz. Whereas other transducers, with vertical tubings, indicated acceptable dynamic responses.
- 3) A modified transducer mounting scheme, which allows natural venting of air bubbles, with a shortened tubing was tested. The evaluated dynamic response was satisfactory up to 200 Hz.
- 4) All the pool boundary (bottom and wall) transducers were modified. Also the pressure tubings of the vent pipe transducers were shortened. The modification was completed before TEST 3103.
- 5) The tests indicated that the cavity-type transducer is fairly sensitive

to acceleration of itself. Extreme care should be taken when it is installed at the locations where mechanical vibration is expected.

Acknowledgements

The present evaluation test was conducted by the member the CRT Technical Group: T. Minori, Y. Miyamoto, T. Chiba, H. Itoh, H. Osaki, N. Yamamoto, and M. Tsukamoto.

We are indebted to technical discussions concerning the present work with many engineers and scientists outside JAERI, however, the authors wish to express their thanks especially to: Dr. E.W. McCauley (LLNL), Dr. J. Lehner (BNL), Prof. A.A. Sonin (MIT), Prof. R. Scanlan (Princeton Univ.), Dr. C.J. Anderson (USNRC), Mr. J. Torbeck (GE), Dr. B. Patel (Creare), Dr. M. Arinobu (Toshiba) and Mr. M. Utamura (Hitachi).

References

- 1) Namatame, K. et al. "Full-Scale Mark 11 CRT Program: Facility Description Report," JAERI-M 8780, March 1980.
- 2) Kukita, Y. et al., "Full-Scale Mark 11 CRT Program: Data Report No.1 TEST 0002," JAERI-M 8598, November, 1979.

to acceleration of itself. Extreme care should be taken when it is installed at the locations where mechanical vibration is expected.

Acknowledgements

The present evaluation test was conducted by the member the CRT Technical Group: T. Minori, Y. Miyamoto, T. Chiba, H. Itoh, H. Osaki, N. Yamamoto, and M. Tsukamoto.

We are indebted to technical discussions concerning the present work with many engineers and scientists outside JAERI, however, the authors wish to express their thanks especially to: Dr. E.W. McCauley (LLNL), Dr. J. Lehner (BNL), Prof. A.A. Sonin (MIT), Prof. R. Scanlan (Princeton Univ.), Dr. C.J. Anderson (USNRC), Mr. J. Torbeck (GE), Dr. B. Patel (Creare), Dr. M. Arinobu (Toshiba) and Mr. M. Utamura (Hitachi).

References

- 1) Namatame, K. et al. "Full-Scale Mark 11 CRT Program: Facility Description Report," JAERI-M 8780, March 1980.
- 2) Kukita, Y. et al., "Full-Scale Mark 11 CRT Program: Data Report No.1 TEST 0002," JAERI-M 8598, November, 1979.

to acceleration of itself. Extreme care should be taken when it is installed at the locations where mechanical vibration is expected.

Acknowledgements

The present evaluation test was conducted by the member the CRT Technical Group: T. Minori, Y. Miyamoto, T. Chiba, H. Itoh, H. Osaki, N. Yamamoto, and M. Tsukamoto.

We are indebted to technical discussions concerning the present work with many engineers and scientists outside JAERI, however, the authors wish to express their thanks especially to: Dr. E.W. McCauley (LLNL), Dr. J. Lehner (BNL), Prof. A.A. Sonin (MIT), Prof. R. Scanlan (Princeton Univ.), Dr. C.J. Anderson (USNRC), Mr. J. Torbeck (GE), Dr. B. Patel (Creare), Dr. M. Arinobu (Toshiba) and Mr. M. Utamura (Hitachi).

References

- 1) Namatame, K. et al. "Full-Scale Mark 11 CRT Program: Facility Description Report," JAERI-M 8780, March 1980.
- 2) Kukita, Y. et al., "Full-Scale Mark 11 CRT Program: Data Report No.1 TEST 0002," JAERI-M 8598, November, 1979.

Table 1 Specifications of tested pressure transducer

Model	Kyowa P53-0236C-10
Measuring range	500 kPa
Maximum overload	150 %
Full-scale output	2.0 mV/V \pm 1 %
Non-linearity	0.3 % F.S.
Hysteresis	0.3 % F.S.
Excitation	10 V AC or DC
Nominal bridge resistance	350 ohm \pm 1 %
Compensated temp. range	0 - 80 °C
Operating temp. range	0 - 100 °C
Thermal zero shift	0.02 % F.S./°C
Thermal sensitivity shift	0.02 % F.S./°C

Table 2 Physical properties of silicon oil

Shinetsu Silicone KF 53 (at 25 °C)

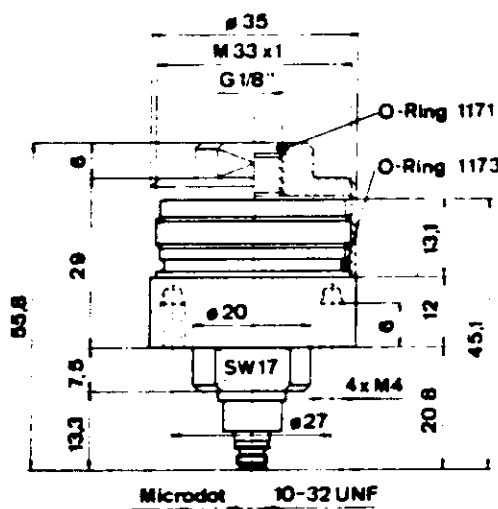
Surface tension	24 - 25 dyne/cm
Viscosity	400 \pm 50 cs
Specific weight	1.06 - 1.08 g/cm ³

Table 3 Specifications of signal conditioner

Model	Kyowa CDA-110AM12
Bridge resistance	120 ohm/350 ohm
Input/Output impedance	2 kohm/10 ohm
Gage factor	2.0
Frequency response	0 - 5 kHz \pm 10 %
L.P.F.*	10, 50, 100, 250 Hz (-3 dB \pm 1 dB) - 12 dB \pm 1 dB/oct.
S/N ratio	51 dB
Zero shift	\pm 0.03 % F.S./ $^{\circ}$ C \pm 0.02 % F.S./hour
Sensitivity shift	\pm 0.02 %/ $^{\circ}$ C \pm 0.16 %/hour

* used at 250 Hz

Table 4 Specifications of reference pressure transducer



Model		7261
Measuring range	bar	-1 -10
Resolution	bar	$15 \cdot 10^{-5}$
Sensitivity	pC/bar	2200
Resonant frequency	kHz	≈ 13
Linearity	%FSO	$< \pm 0.8$
Hysteresis	%FSO	< 0.5
Dead volume	cm	1.5
Volume change	mm ³ ·bar	2.5
Insulation resistance	Ω	$> 5 \cdot 10^{13}$
Capacitance	pF	24
Acceleration sensitivity	bar/g	$< 10^{-3}$
Temperature coefficient of sensitivity	%/°C	-0.02
Temperature error	bar/°C	0.015
Operating temperature range	°C	-40 -240

Table 5 Specifications of charge amplifier, Kistler

Measuring ranges	pC	$\pm 10 - \pm 500,000$
Transducer sensitivity	pC/M.U.	0.1 - 11,000
Output voltage	V	± 10
Insulation resistance at input	T Ω	≈ 100
Frequency range, with standard filter (-3 dB)	kHz	$\approx 0 - 180$
Linearity	%	$< \pm 0.05$

Table 6 Specifications of accelerometer

Model	Bruel & Kjaer, Type 4370
Weight*	54 grams
Voltage sensitivity	≈ 10 mV/ms ⁻²
Charge sensitivity	10 ± 2 % pC/ms ⁻²
Mounted resonance	18 kHz
Frequency range	0.2~3500 (5%), 0.2~6000 (10%)
Max. transverse sensitivity	< 4 %
Piezoelectric Material	PZ23
Construction	Delta Shear

Table 7 Specifications of charge amplifier, Bruel & Kjaer

Model	Bruel & Kjaer, Type 2651
Sensitivity (with 1 nF transducer)	Selectable 0.1-1-10 mV/pC (-20 dB to +20 dB)
Typical rise time	1.5 v/ μ s
Frequency range	3 mHz to 200 kHz LLF selectable 0.003, 0.03, 0.3, 1 Hz, -3 dB
Input impedance	> 10 G Ω
Maximum input	1×10^5 pC
Maximum output	10 V (10 mA) pk
Output DC offset	± 30 mV Dual Supply, +12 V Single Supply
Noise	< 10 μ V (1 Hz ~ 22 kHz)

Table 8 Specifications of DC amplifier, Toyoda

Model	Toyoda AA 1130
Input level	0 - 1.0 V
Maximum output	± 5 V, ± 50 mA
Gain	100 - 2000
Frequency range	DC - 10 kHz, deviation less than 1 dB
Input resistance	>100 kohm
Linearity	<0.5 %

Table 9 Specifications of DC amplifier, Kyowa

Model	Kyowa DA-110AM7		
Frequency range	0 - 20 kHz for 10 Vpp output 0 - 10 kHz for 20 Vpp output		
L.P.F.*	10, 50, 100, 250, -12 dB/oct.		
Gain	100 - 2000, Att. 1 - 1/2.5		
Gain stability	<0.01 %		
Gain accuracy	<0.1 %		
Input/Output impedance	>20 Mohm/<0.1 ohm		
CMRR	>120 dB for 0 - 60 Hz		
Output	>10 V		
Temp. drift	< $\pm(3 \mu\text{V}/^\circ\text{C RTI} + 0.1 \text{ mV}/^\circ\text{C RTD})$ for zero input		
Noise	L.P.F.	Noise level	
	1000 Hz	<8 μVpp ,	<1 μVrms
	100 Hz	<3 μVpp ,	
Non-linearity	<0.01 %		

* not used

Table 10 Test matrix, original transducers

Test No.	Transducer	System press. (kPa)	Fig. No.
PT 9251	Wall	350	10 and 11
PT 9252	Wall	250	12 " 13
PT 9253	Wall	150	14 " 15
PT 9271	Bottom	350	16 " 17
PT 9272	Bottom	250	18 " 19
PT 9273	Bottom	150	20 " 21
PT 9274	Bottom*	350	22 " 23

* 'Air free' test

Table 11 Test matrix, modified transducer

Test No.	Transducer	System press. (kPa)	Fig. No.
PT 9261	Modified pool boundary	350	26 and 27
PT 9262	Modified pool boundary	250	28 " 29
PT 9263	Modified pool boundary	150	30 " 31

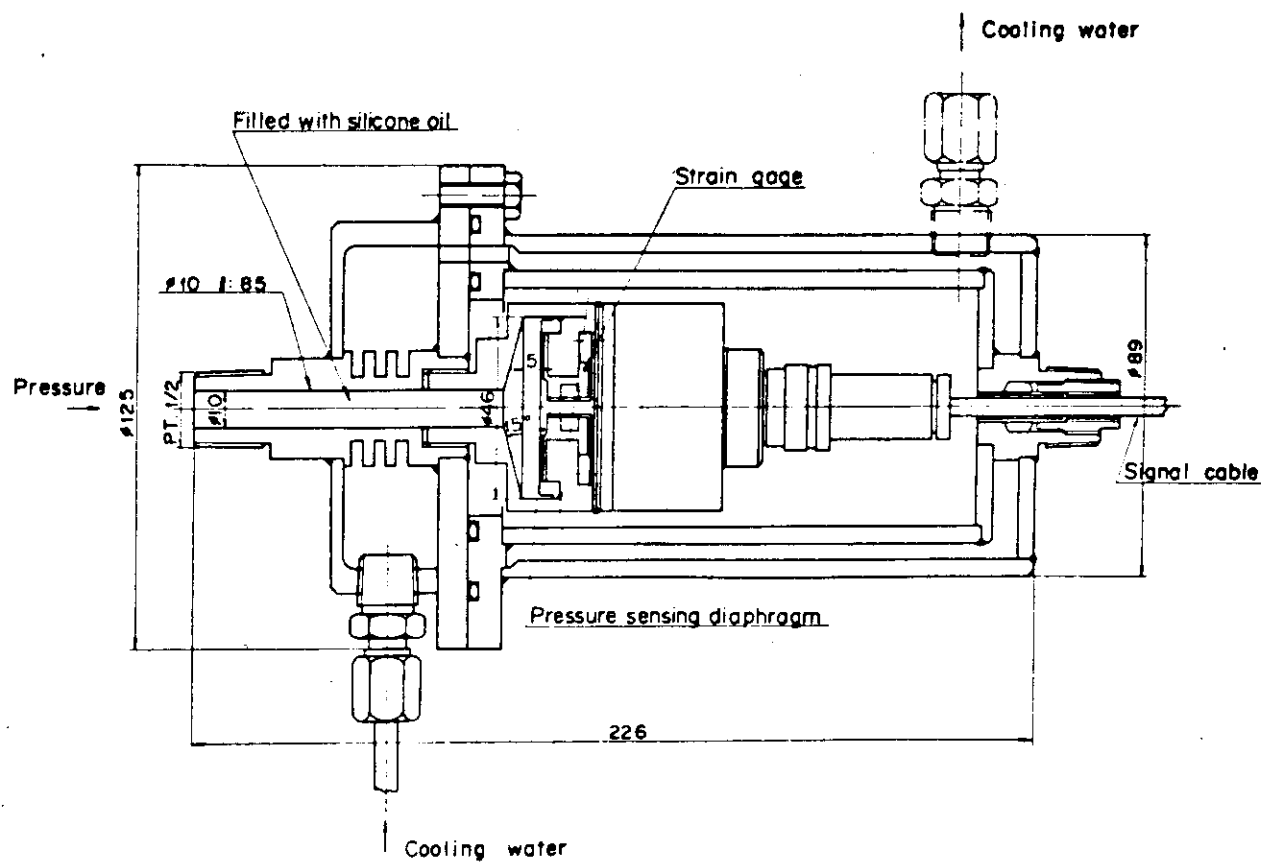


Fig. 1 Cross-section of cavity-type pressure transducer

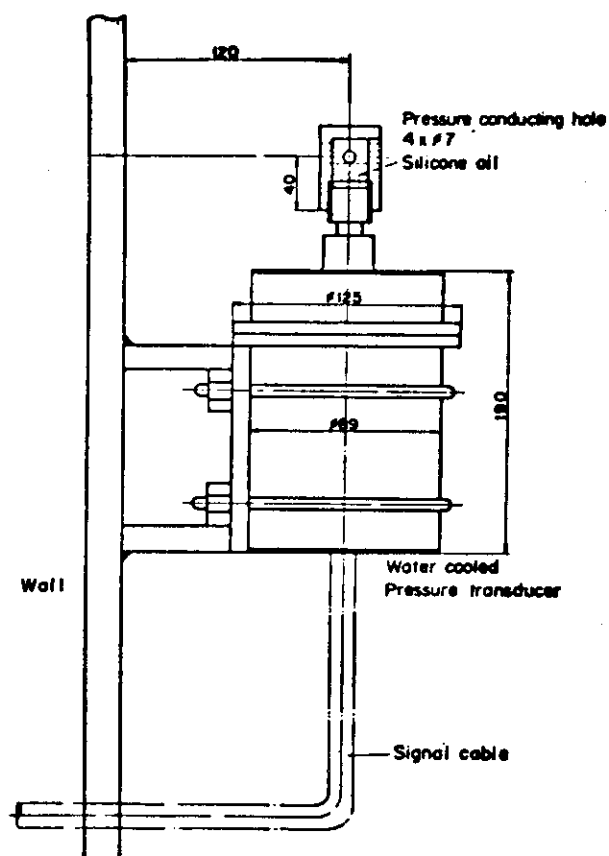


Fig. 2 Pressure transducer installation scheme:
wall pressure transducer

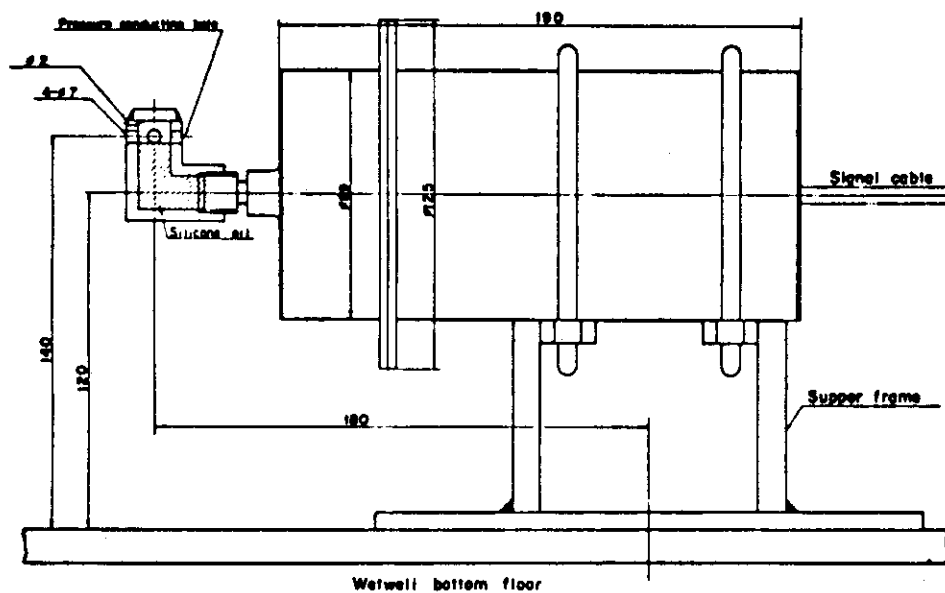


Fig. 3 Pressure transducer installation scheme:
wall pressure transducer (before modification)

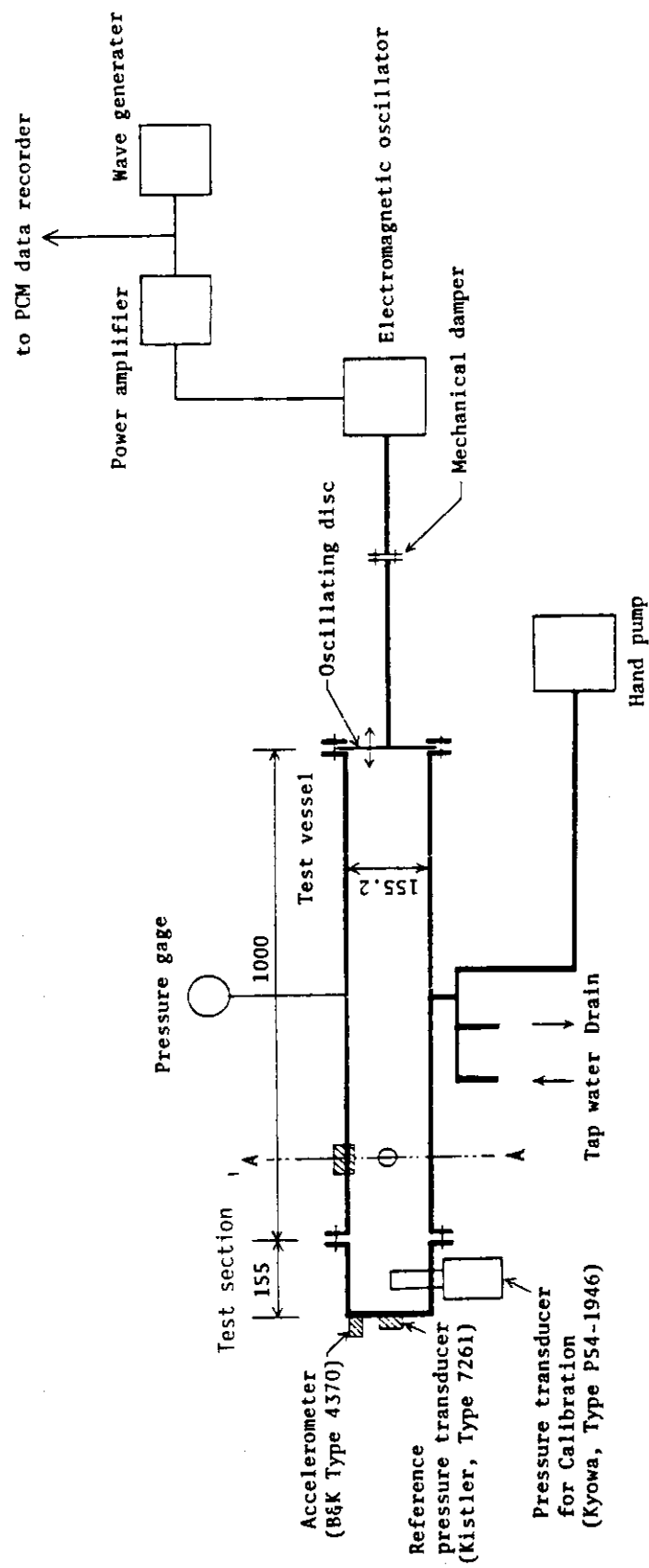


Fig. 4 Schematic of test apparatus

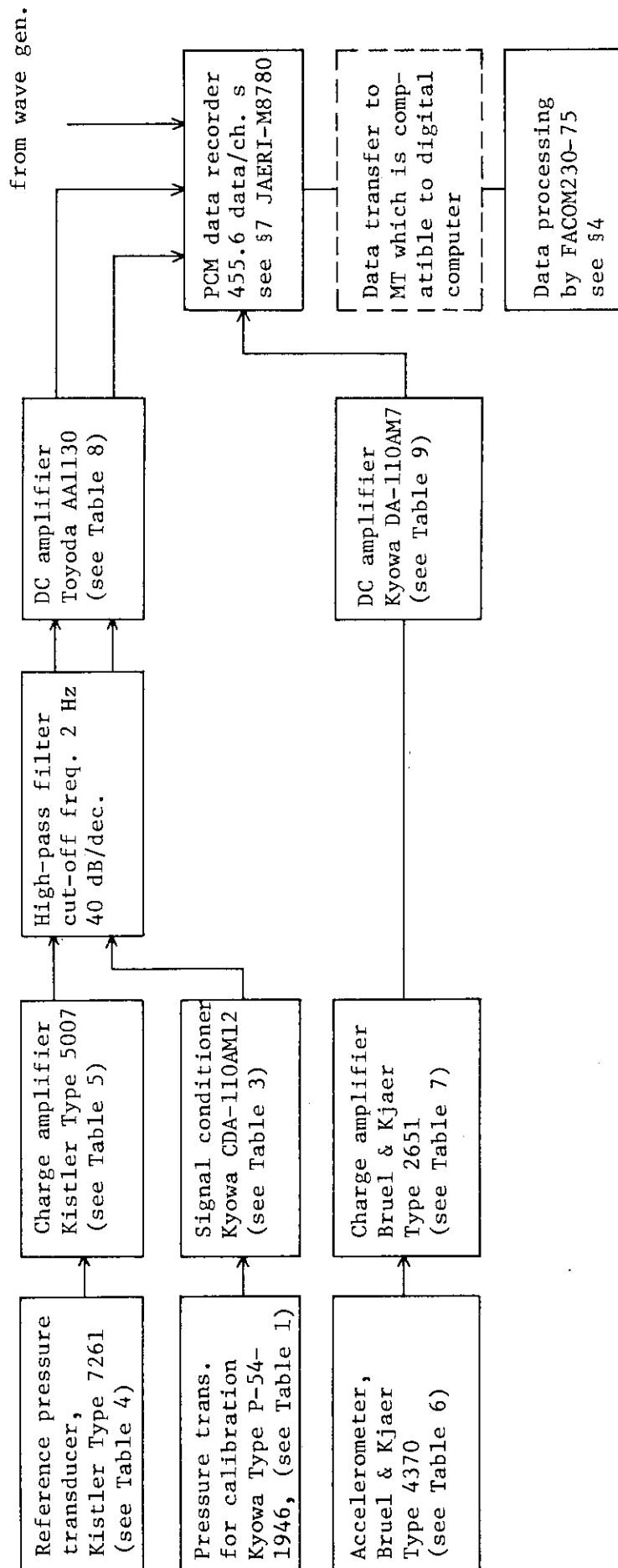


Fig. 5 Block diagram of test equipments

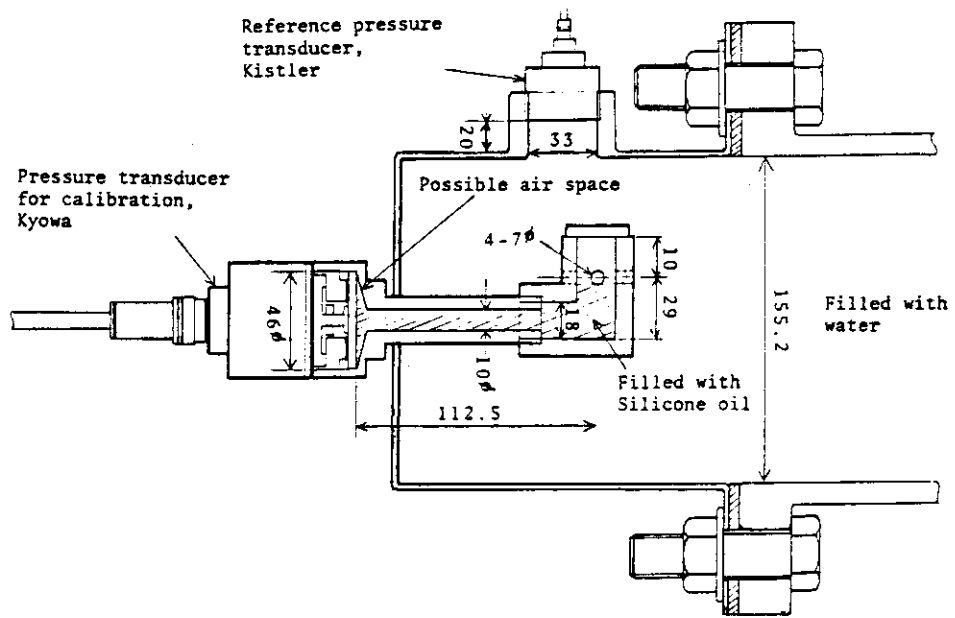


Fig. 6 Test arrangement for bottom transducer

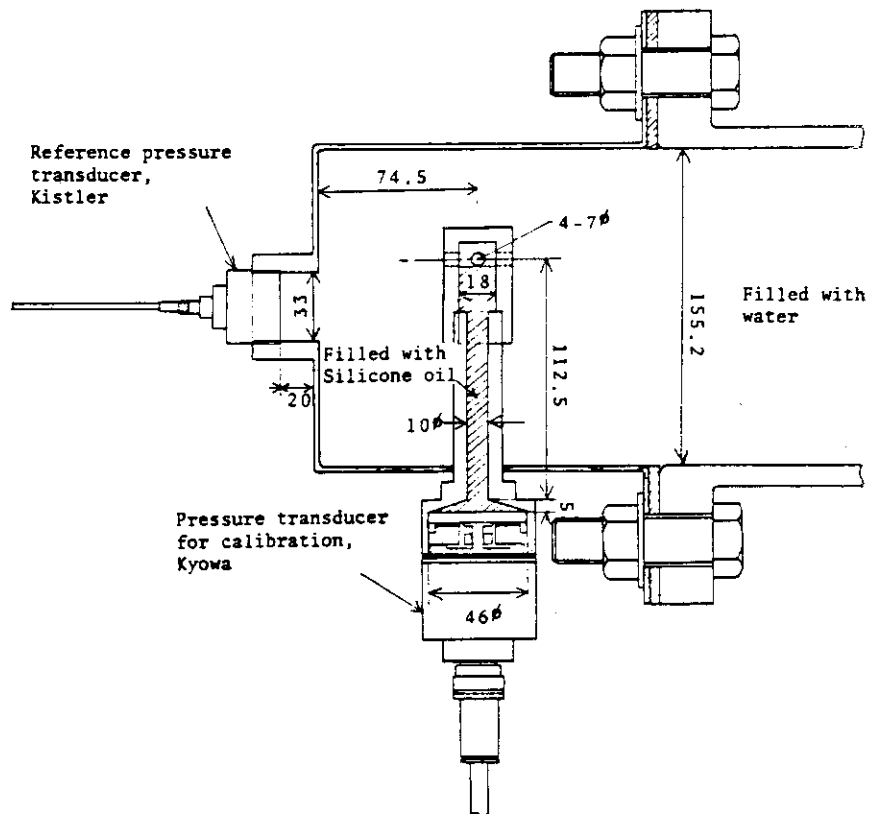


Fig. 7 Test arrangement for wall transducer

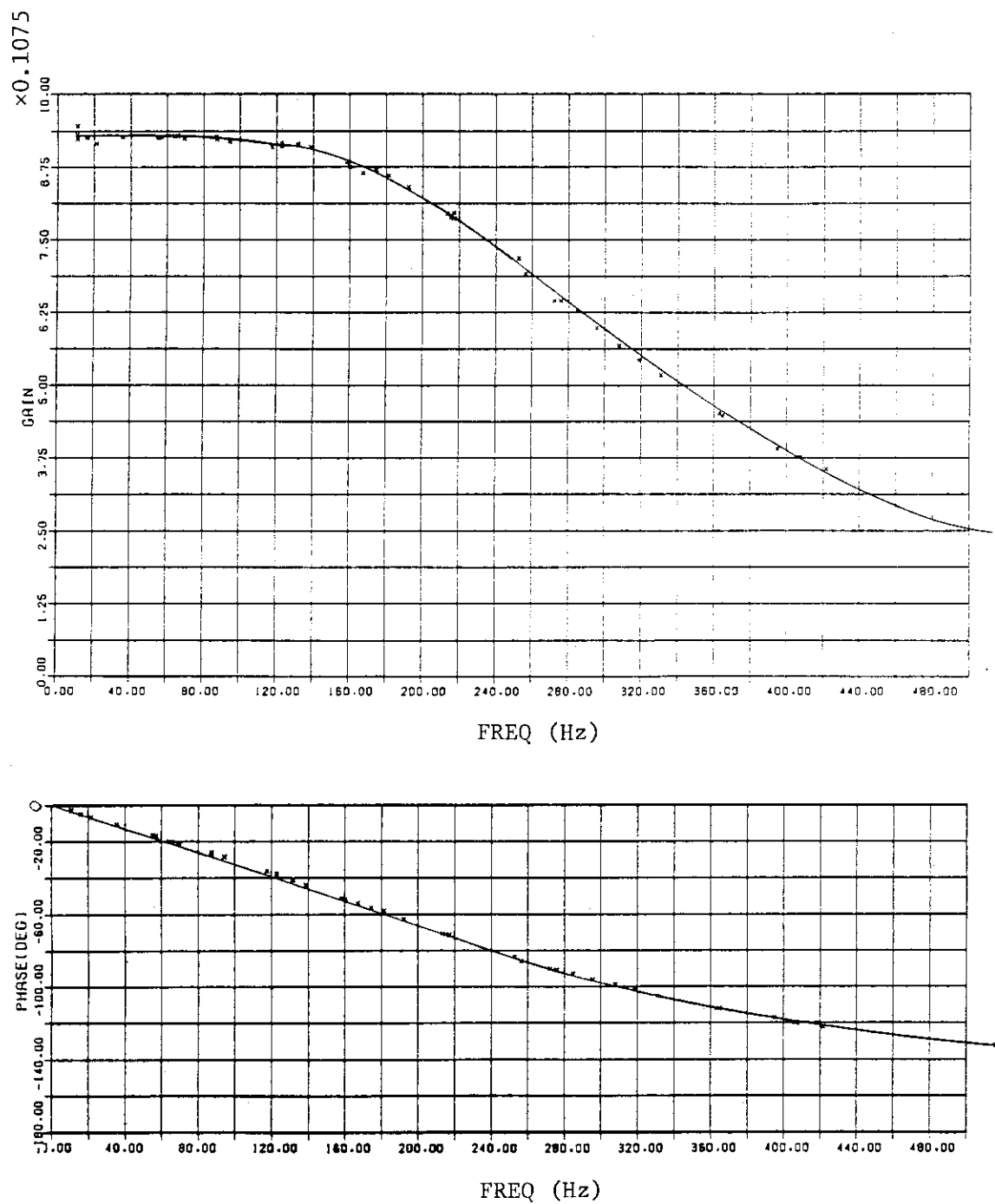


Fig. 8 Gain and phase characteristics of built-in low-pass filter of Kyowa signal conditioner.
(Nominal cut-off frequency = 250 Hz)

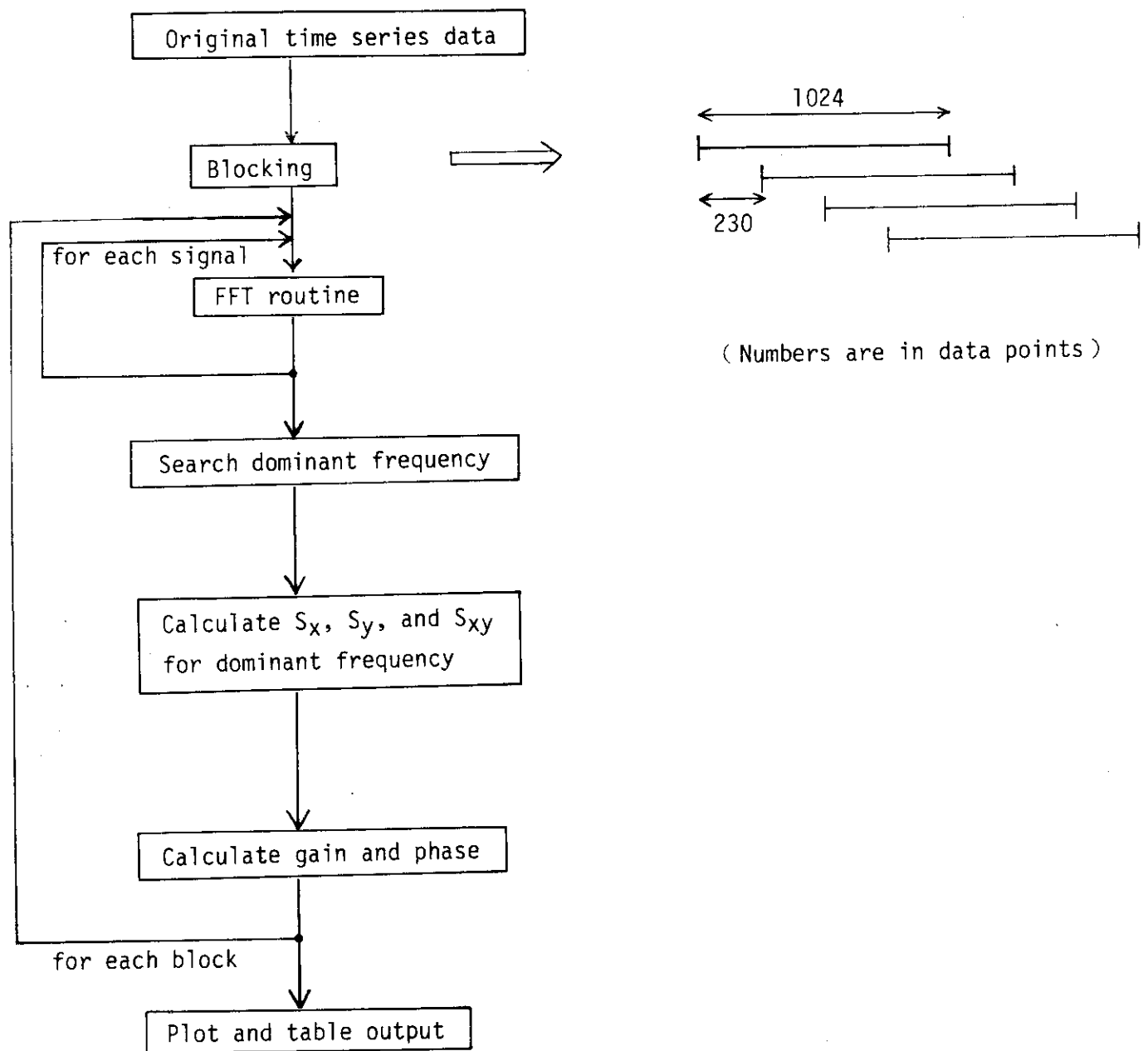


Fig. 9 Block diagram of data-processing computer program

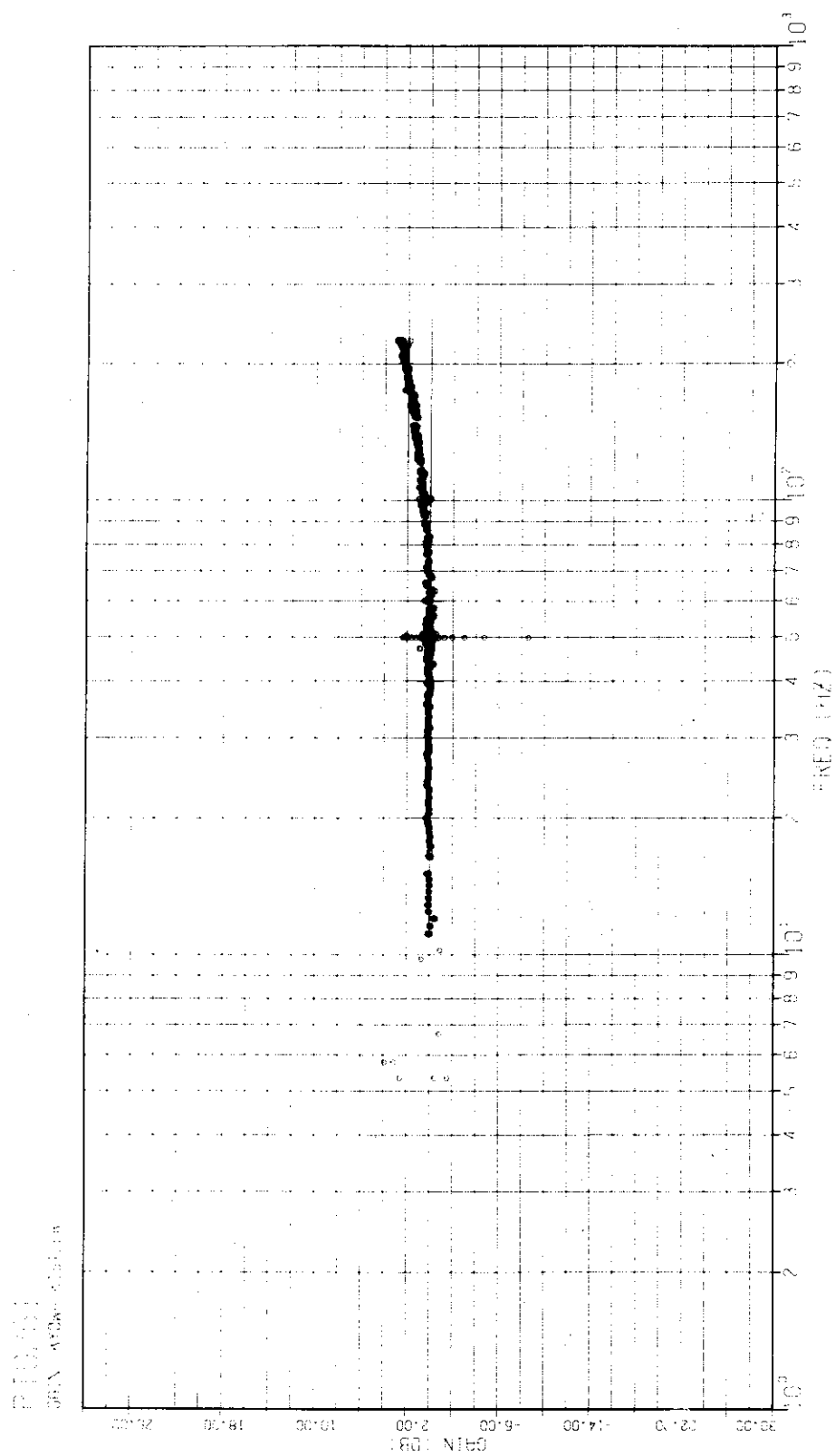


Fig. 10 Gain response of wall transducer, 350 kPa system pressure

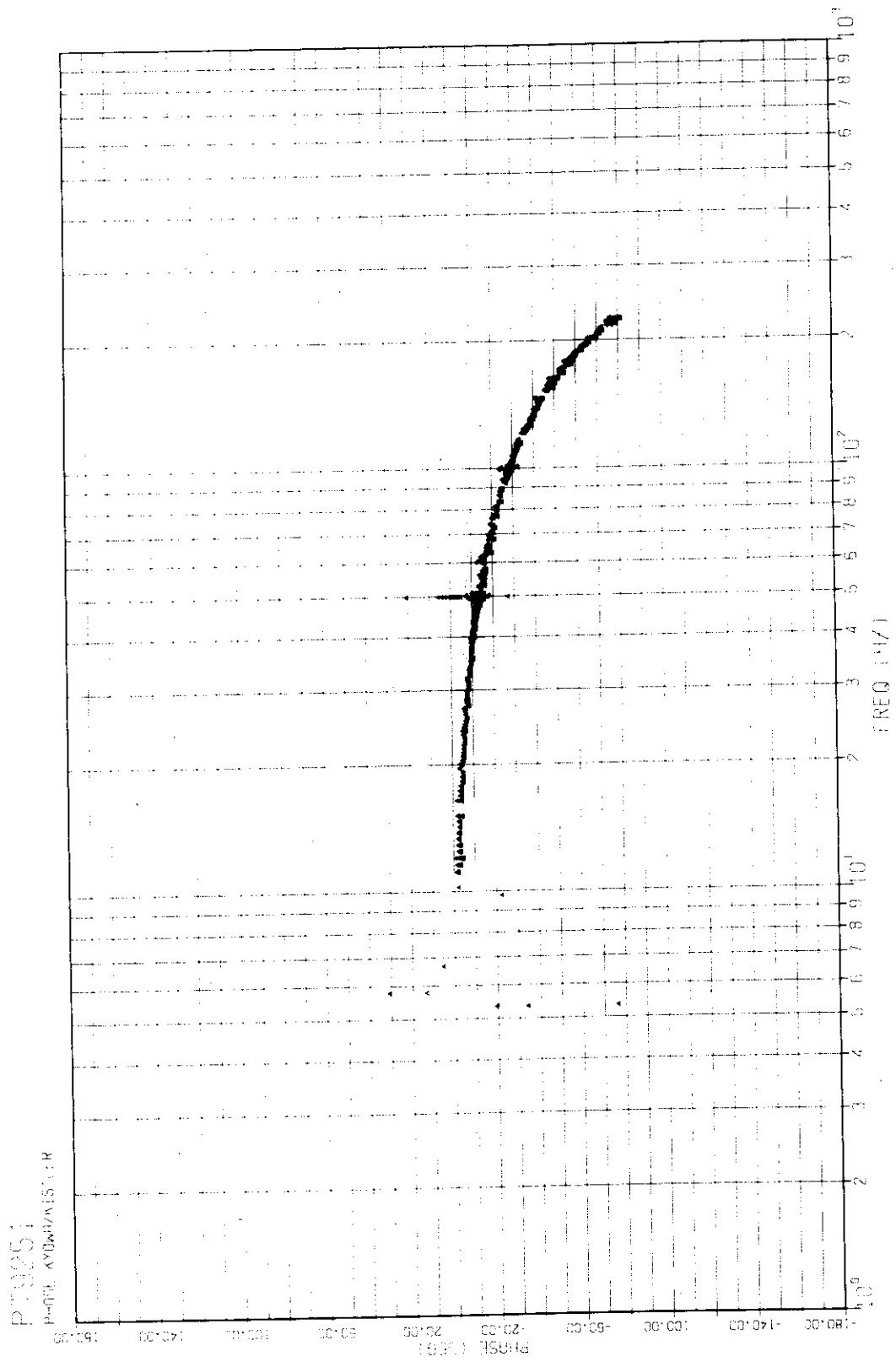


Fig. 11 Phase response of wall transducer, 350 kPa system pressure

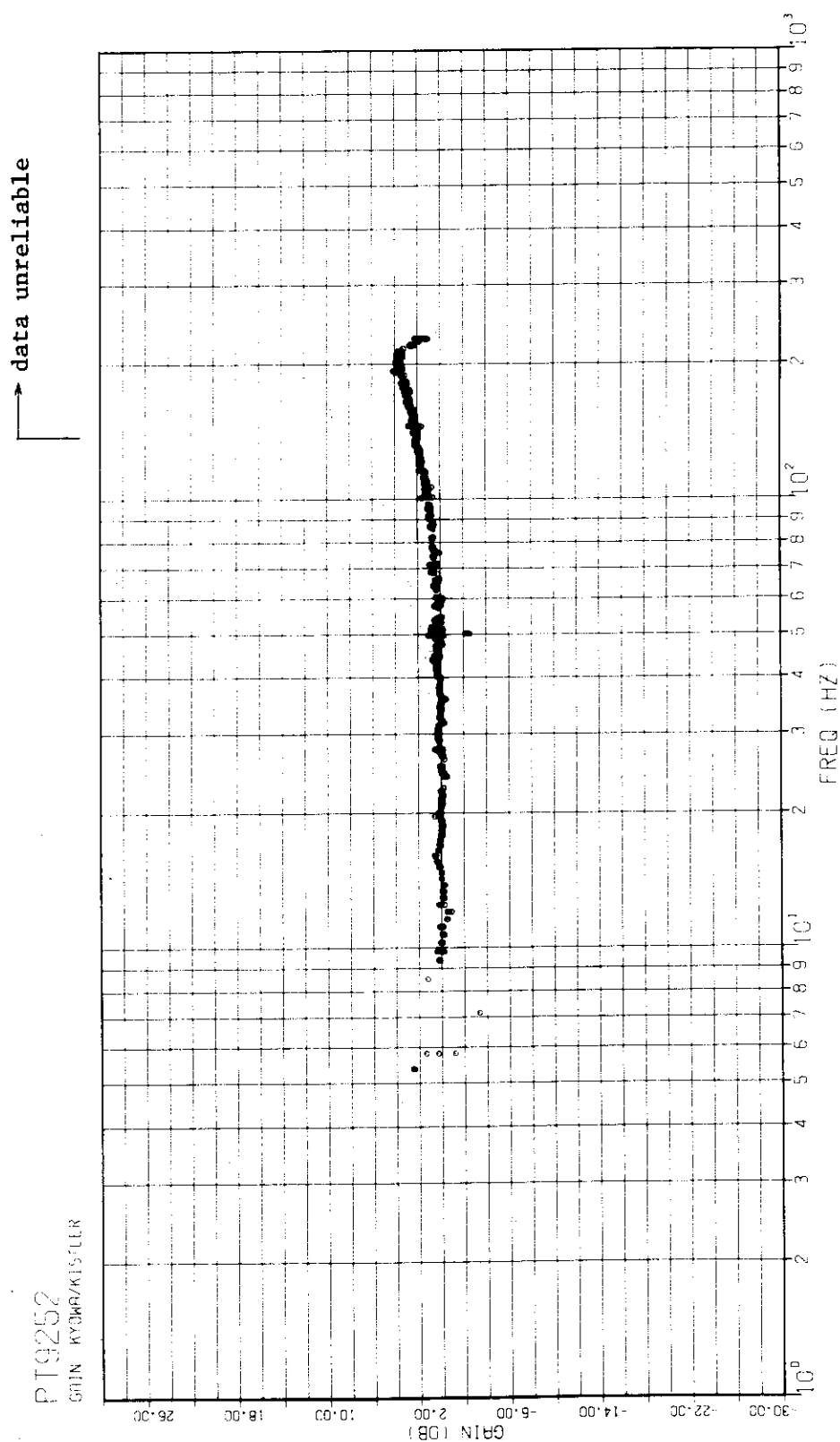


Fig. 12 Gain response of wall transducer, 250 kPa system pressure

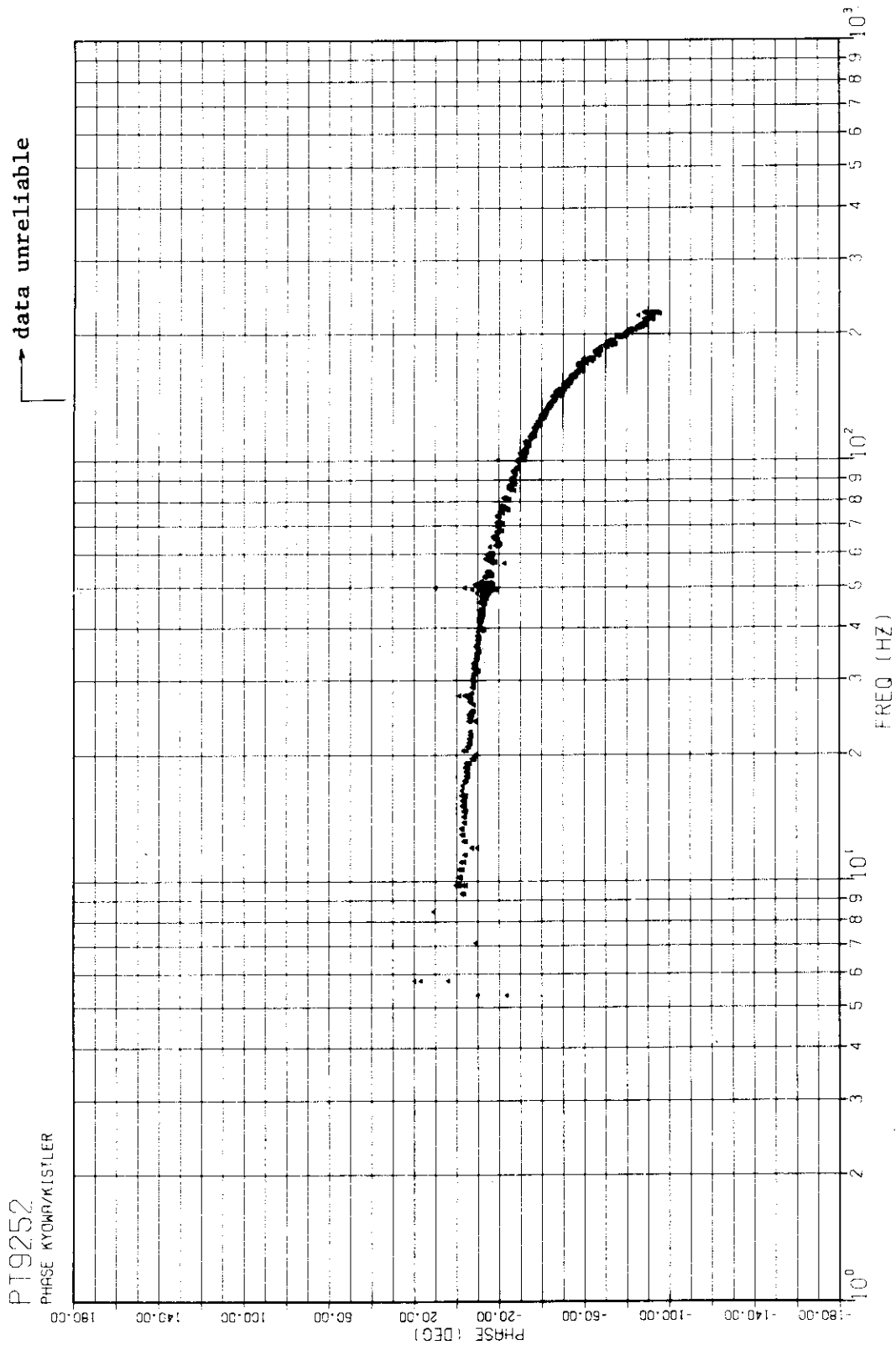


Fig. 13 Phase response of wall transducer, 250 kPa system pressure

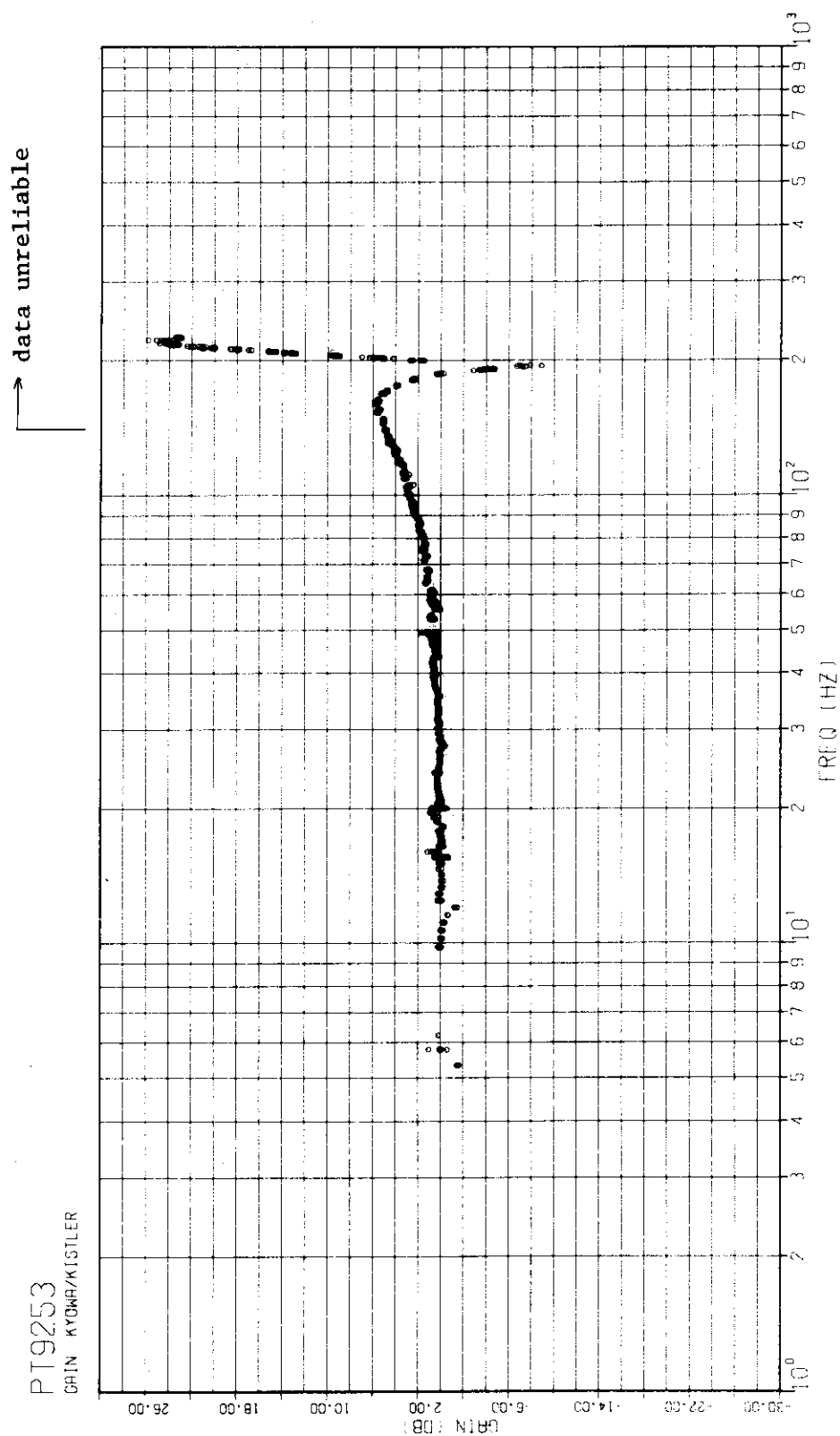


Fig. 14 Gain response of wall transducer, 150 kPa system pressure

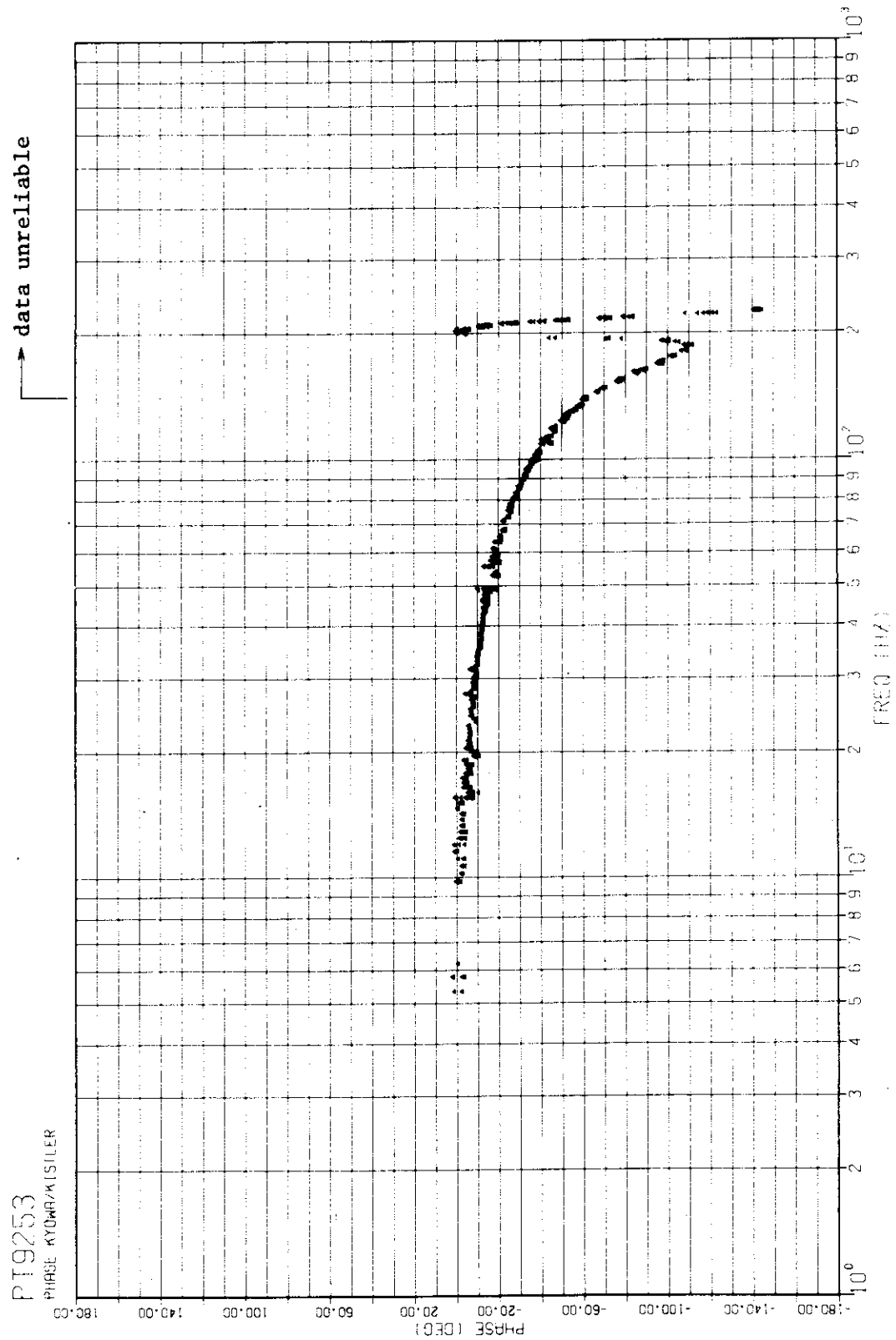


Fig. 15 Phase response of wall transducer, 150 kPa system pressure

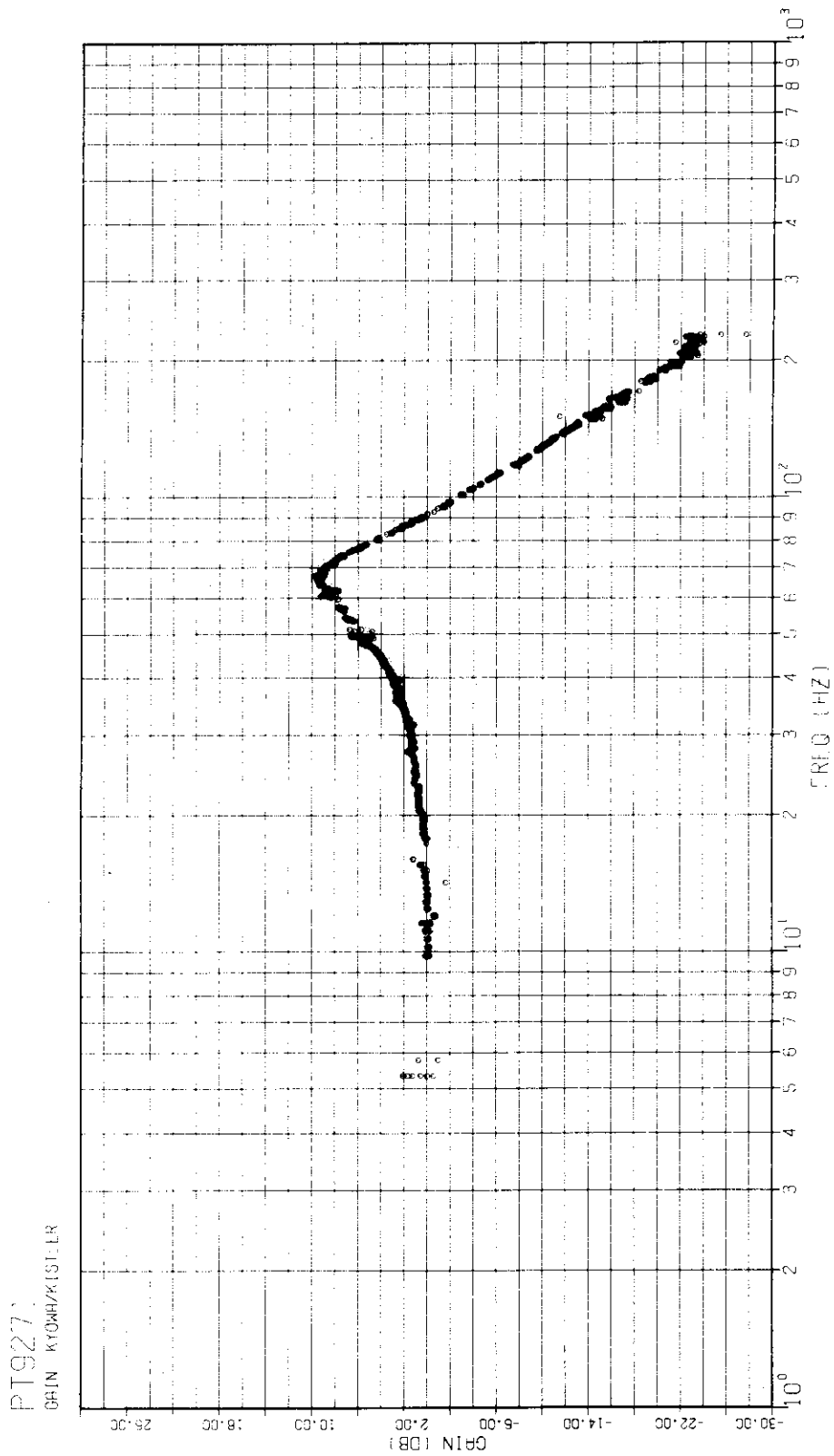


Fig. 16 Gain response of bottom transducer, 350 kPa system pressure

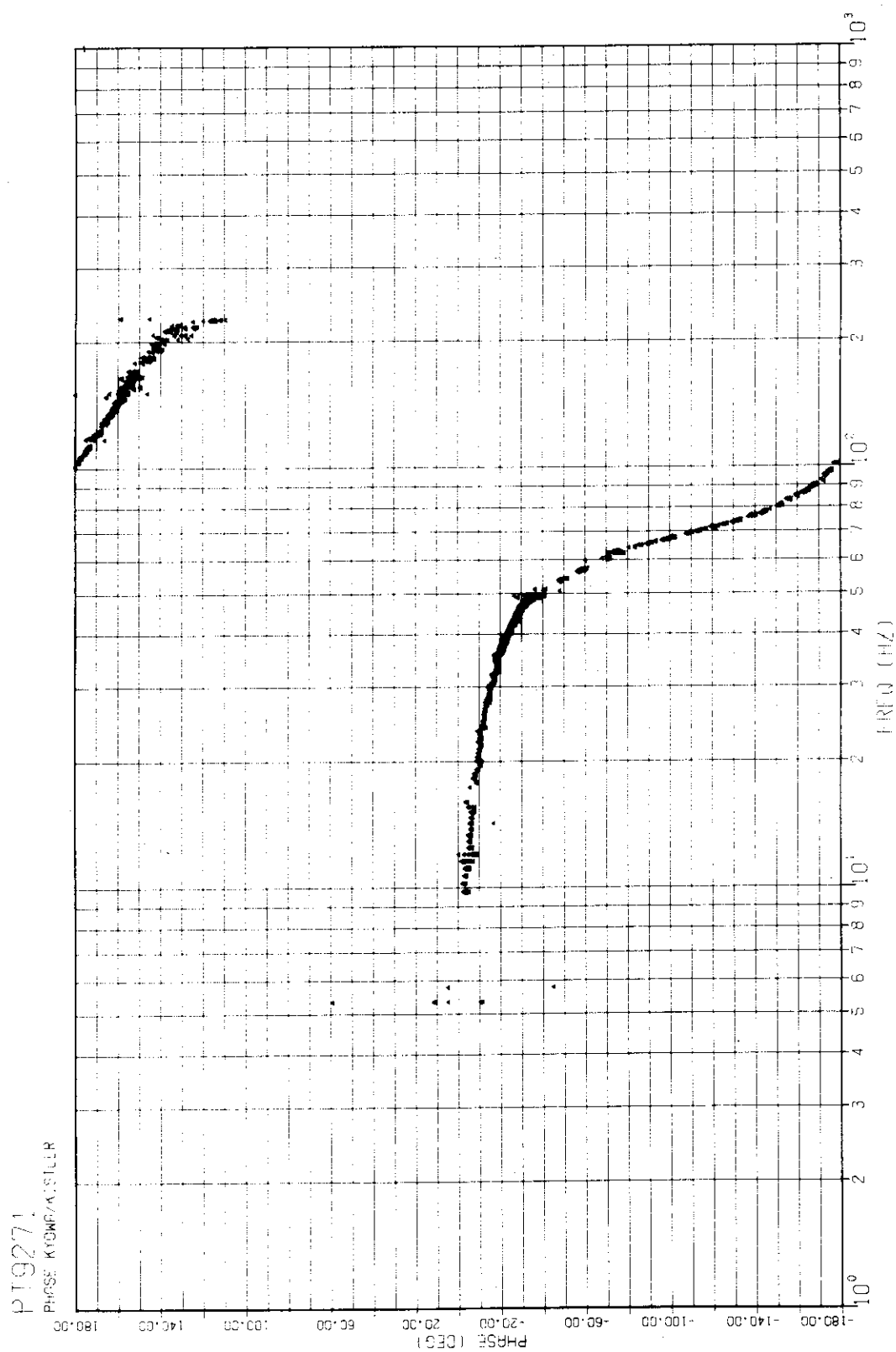


Fig. 17 Phase response of bottom transducer, 350 kPa system pressure

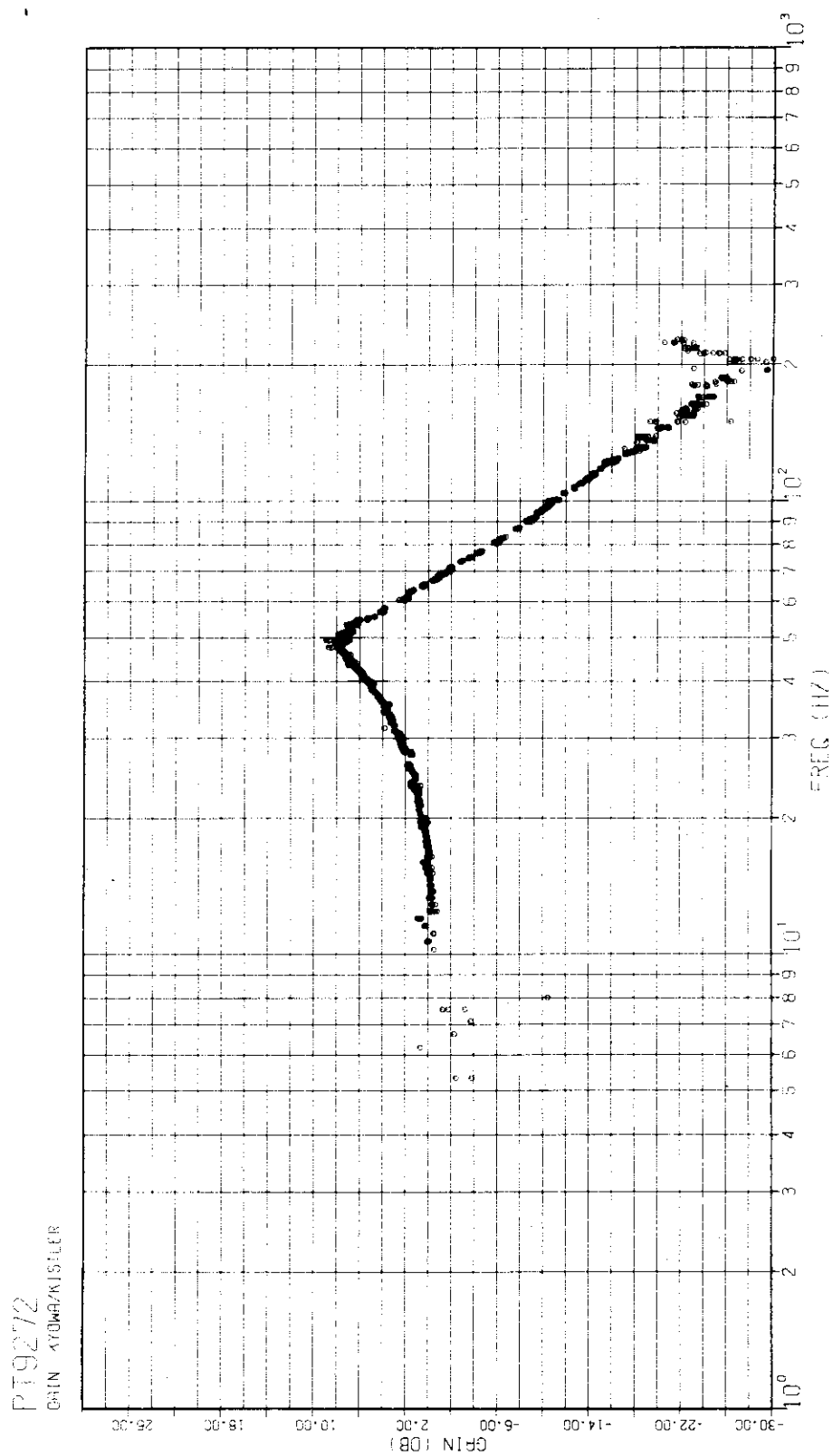


Fig. 18 Gain response of bottom transducer, 250 kPa system pressure

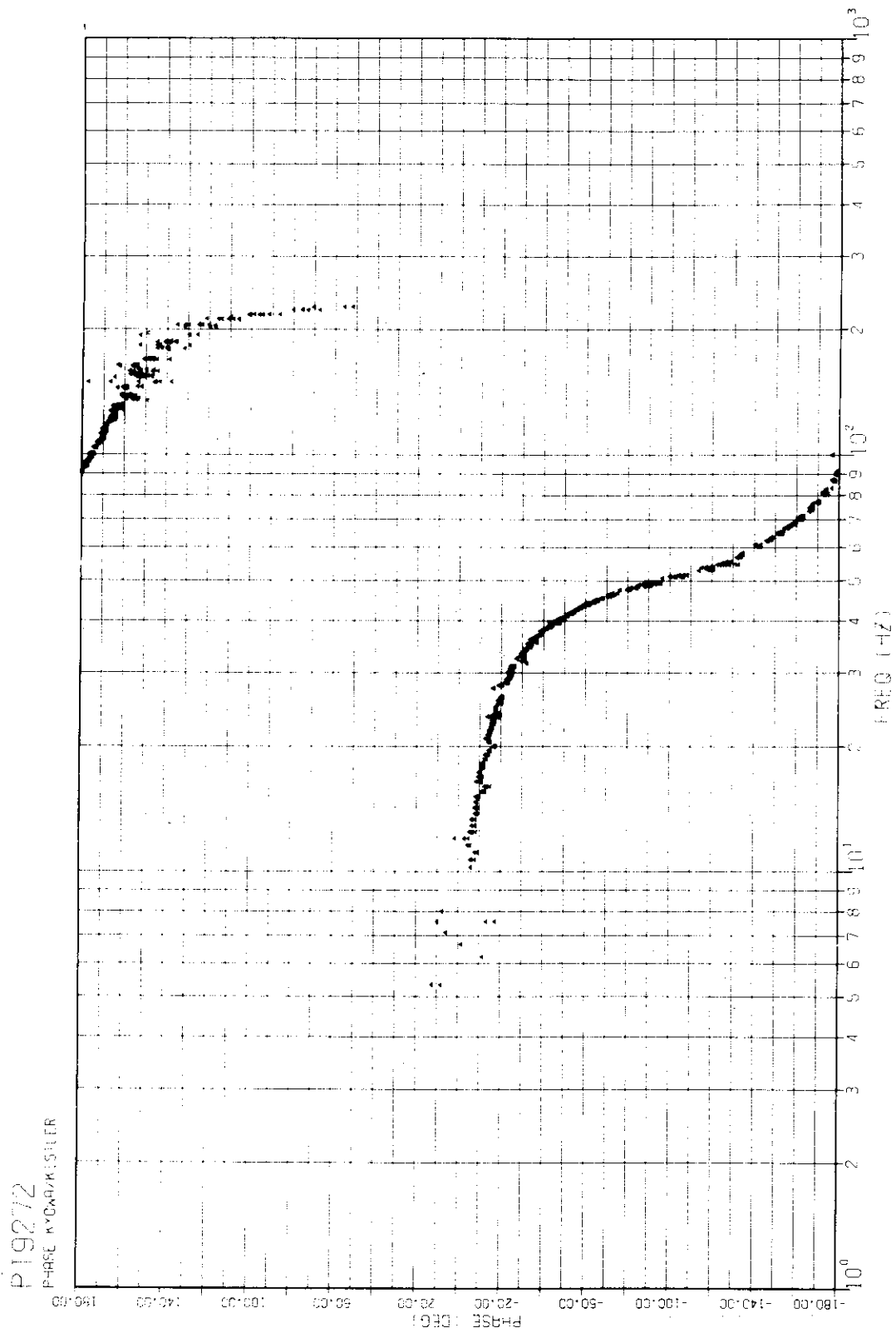


Fig. 19 Phase response of bottom transducer, 250 kPa system pressure

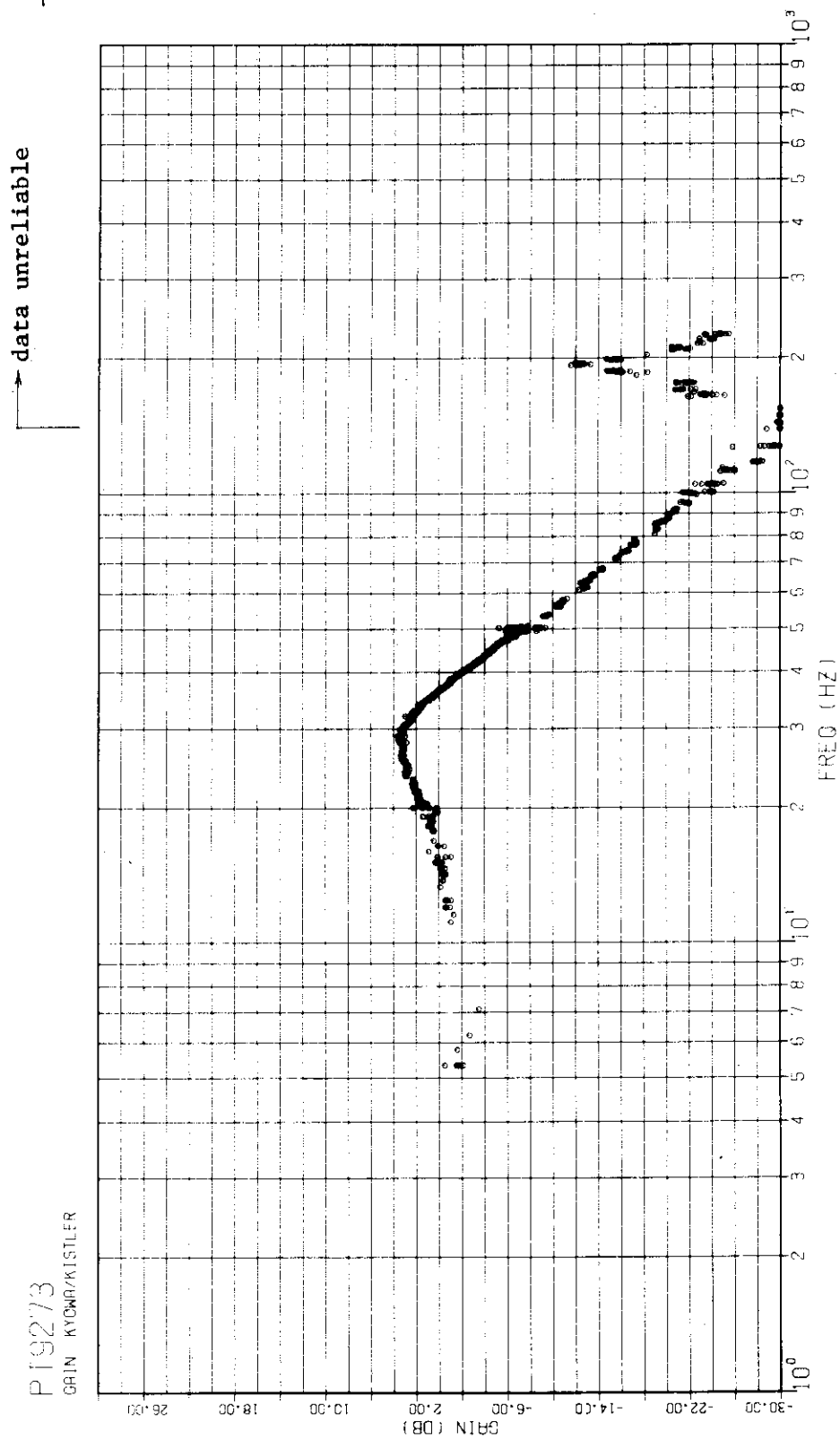


Fig. 20 Gain response of bottom transducer, 150 kPa system pressure

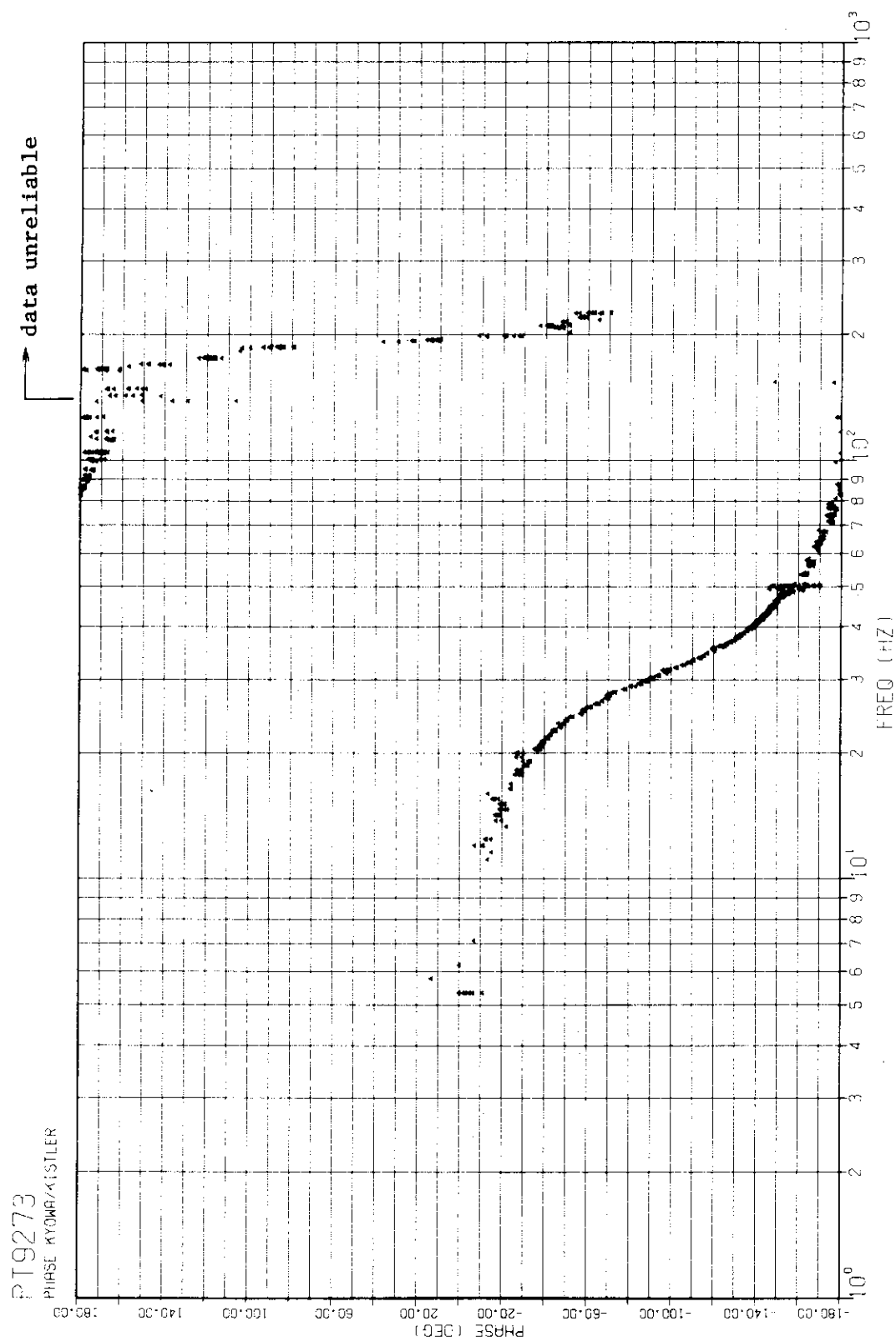


Fig. 21 Phase response of bottom transducer, 150 kPa system pressure

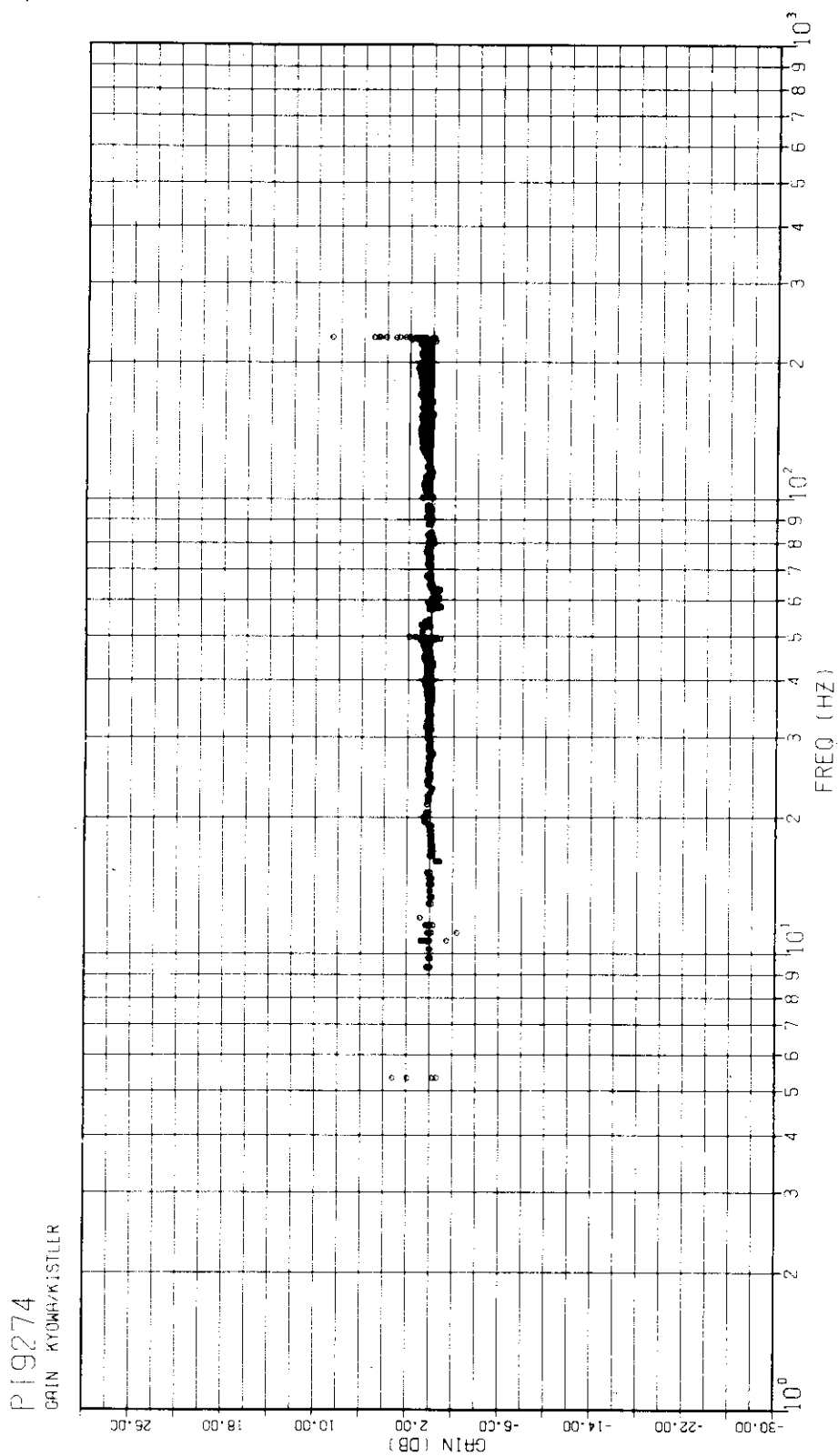


Fig. 22 Gain response of bottom transducer, 350 kPa system pressure 'air free' test

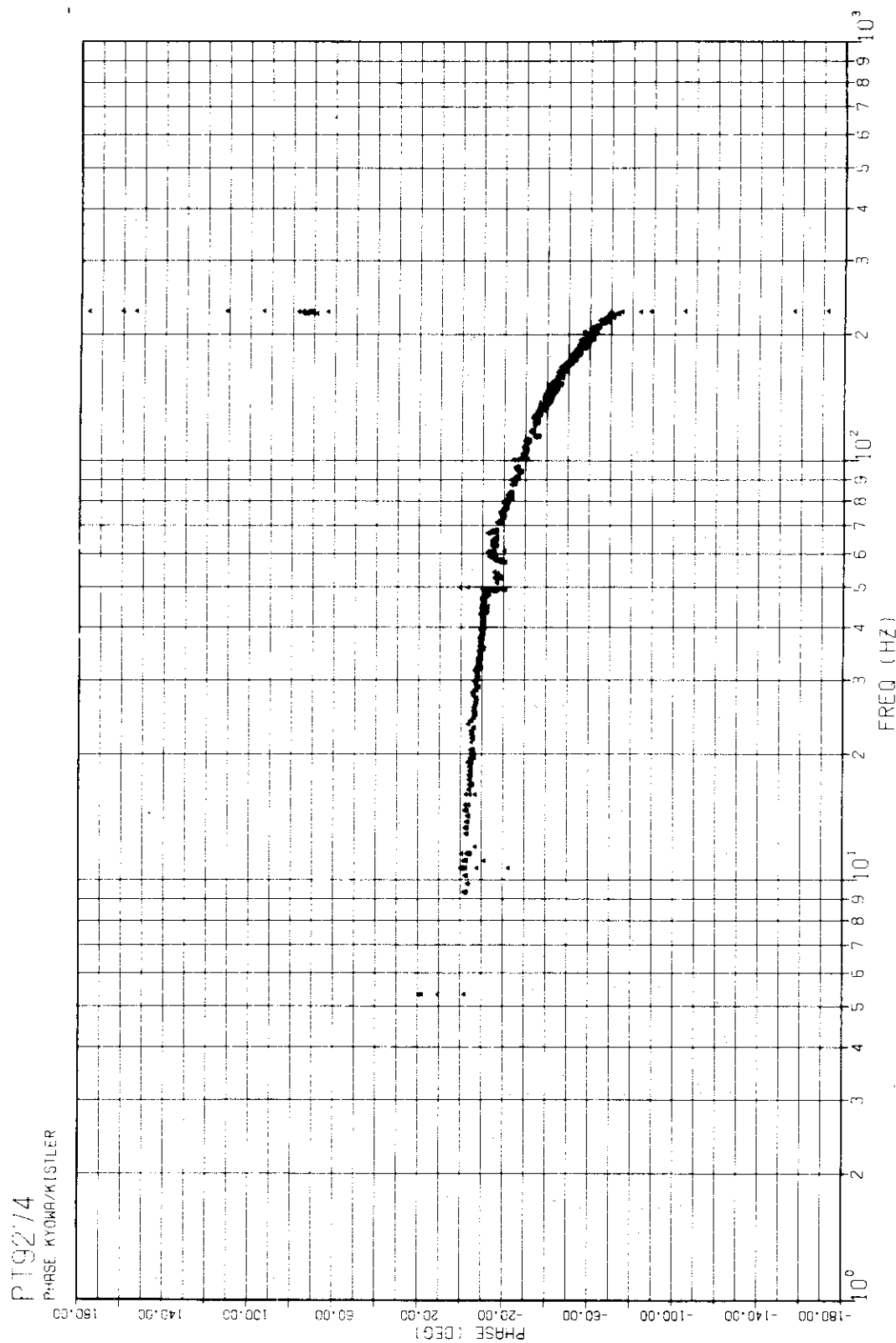


Fig. 23 Phase response of bottom transducer, 350 kPa system pressure 'air free' test

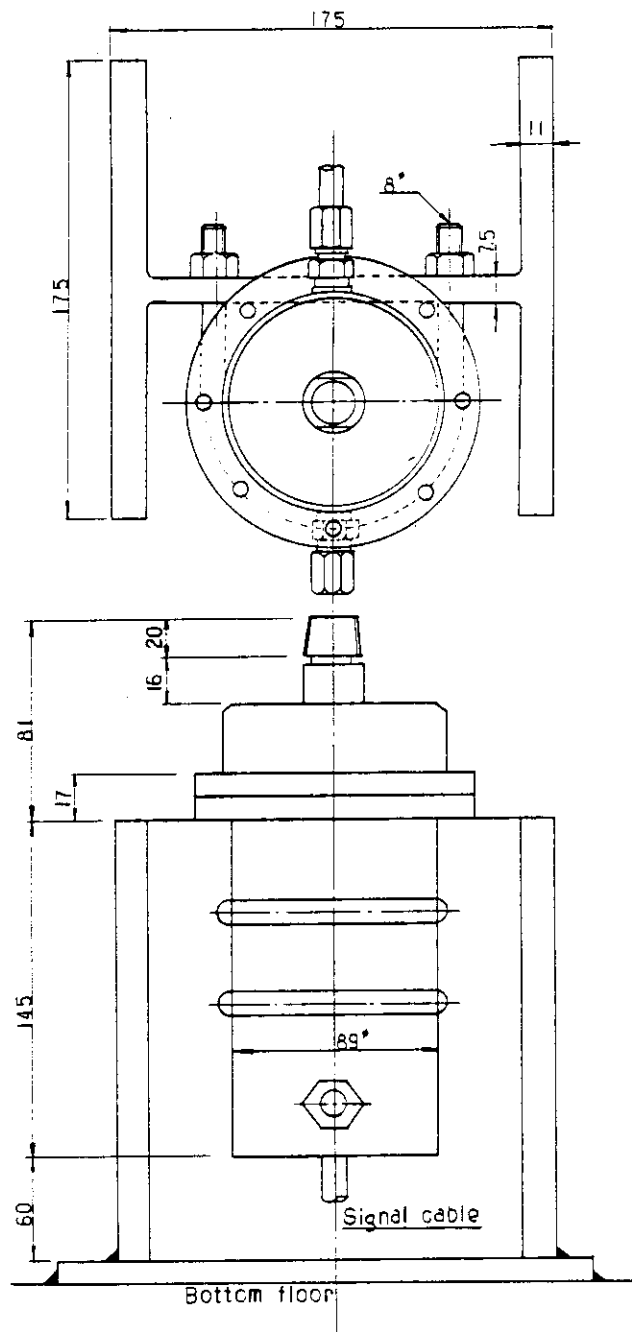
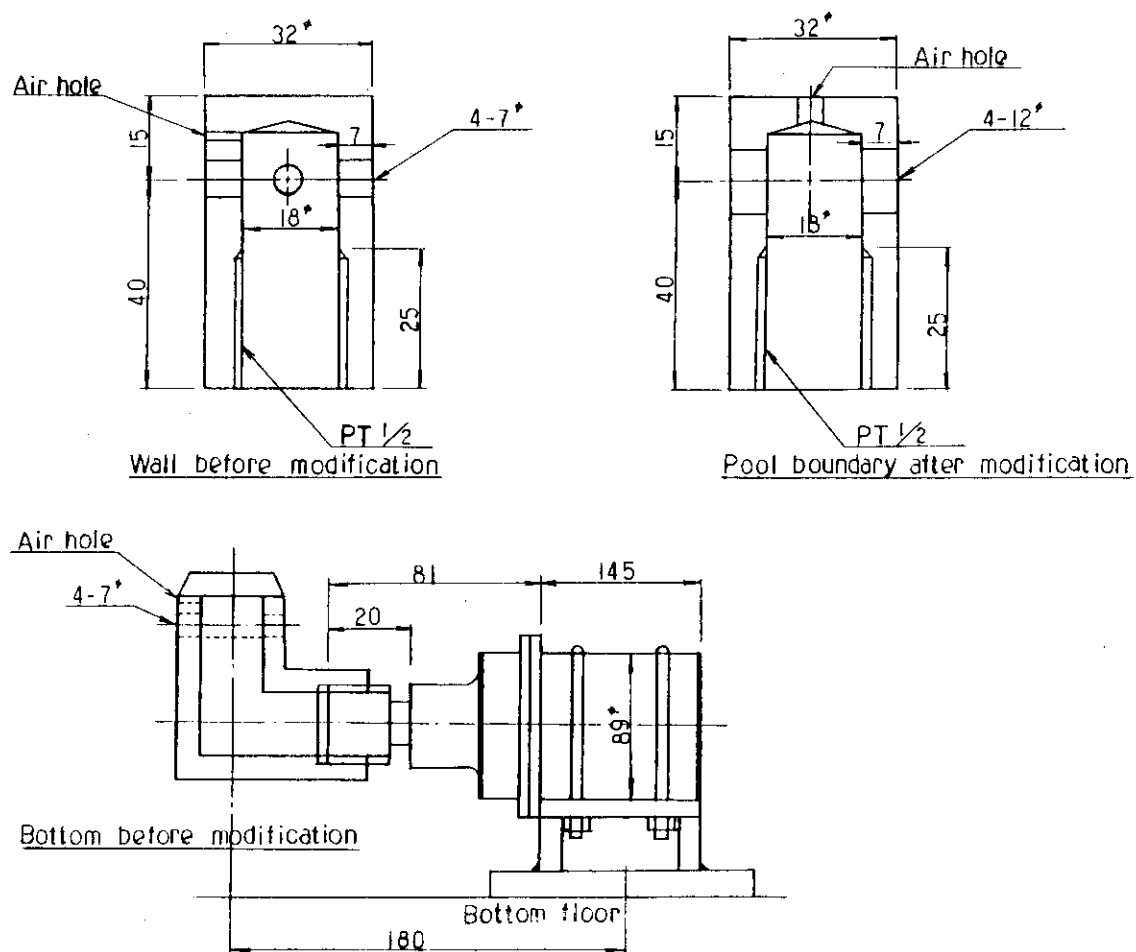


Fig. 24 Modified mounting scheme for bottom transducer



(Not in scale)

Fig. 25 Pressure tubing inlet designs
(Also see Figs. 6 and 7)

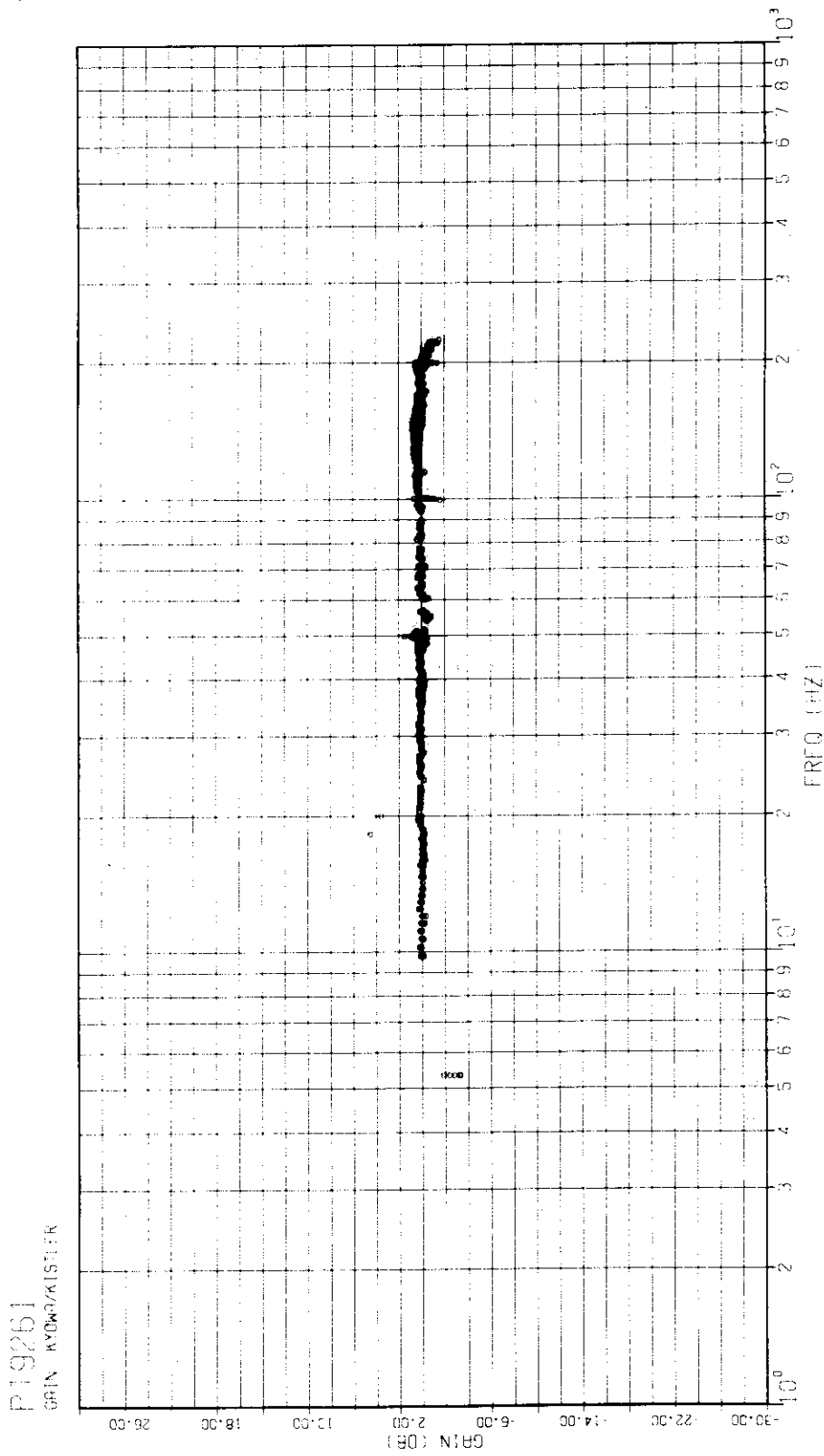


Fig. 26 Gain response of modified transducer, 350 kPa system pressure

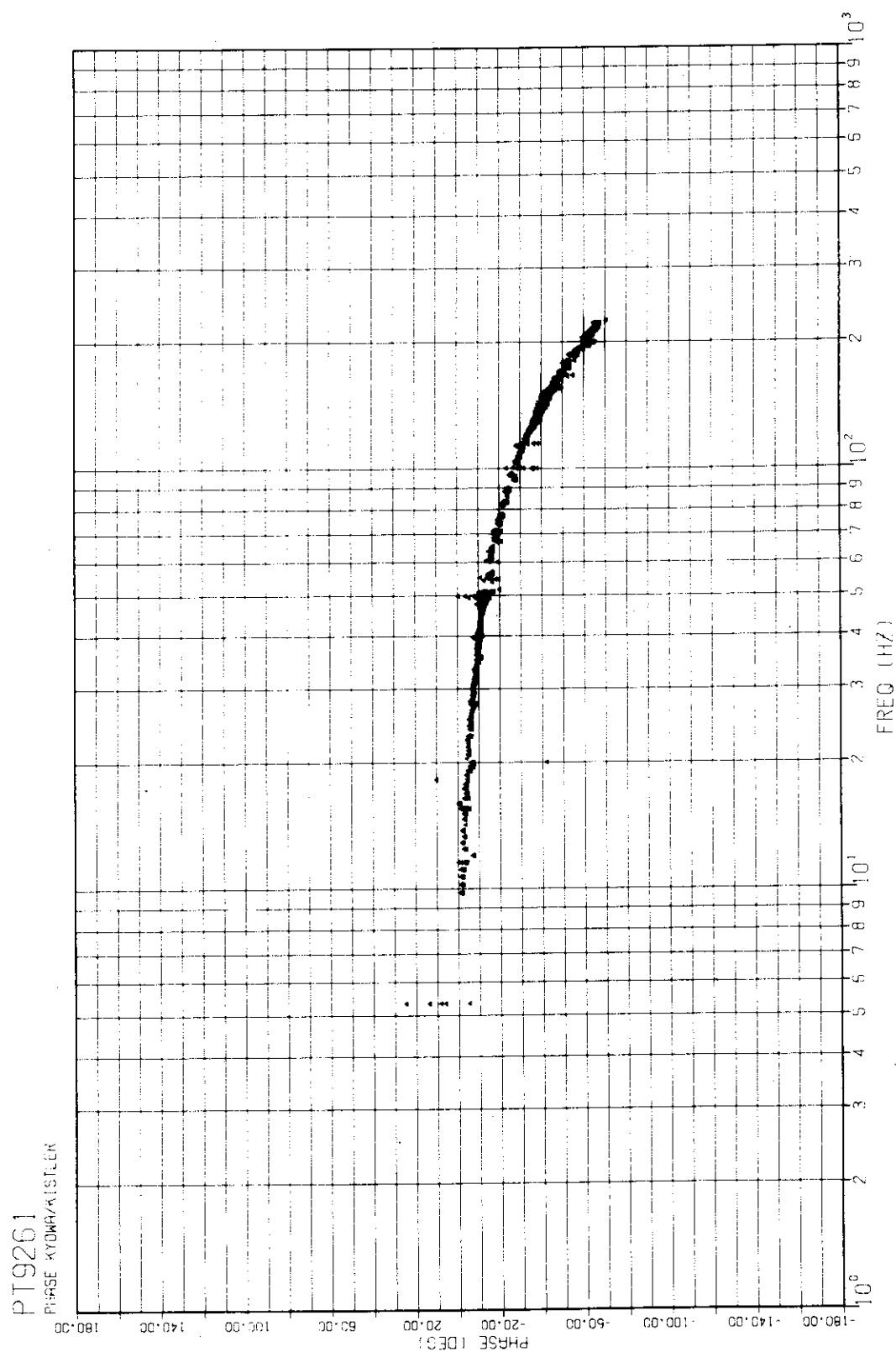


Fig. 27 Phase response of modified transducer, 350 kPa system pressure

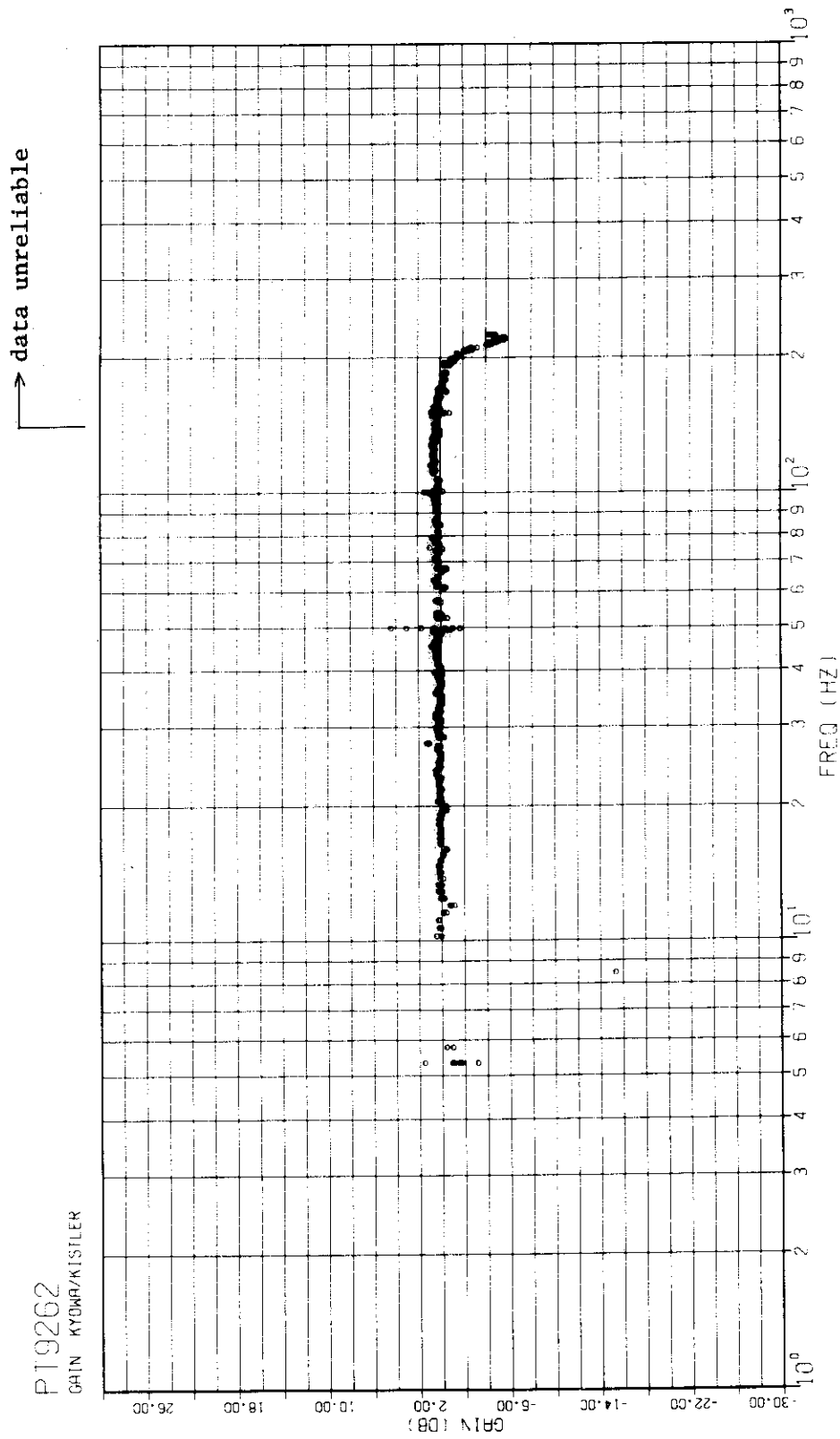


Fig. 28 Gain response of modified transducer, 250 kPa system pressure

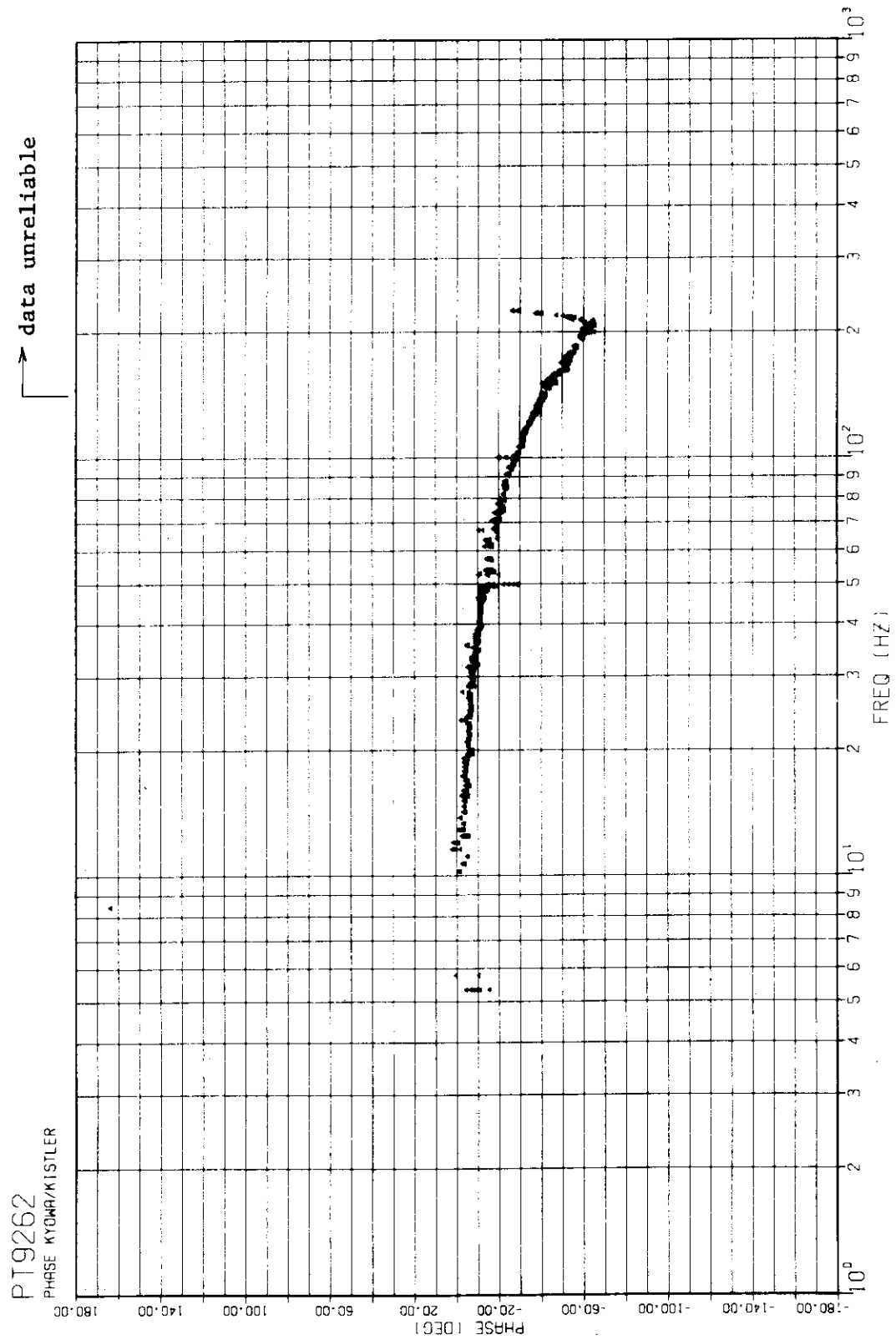


Fig. 29 Phase response of modified transducer, 250 kPa system pressure

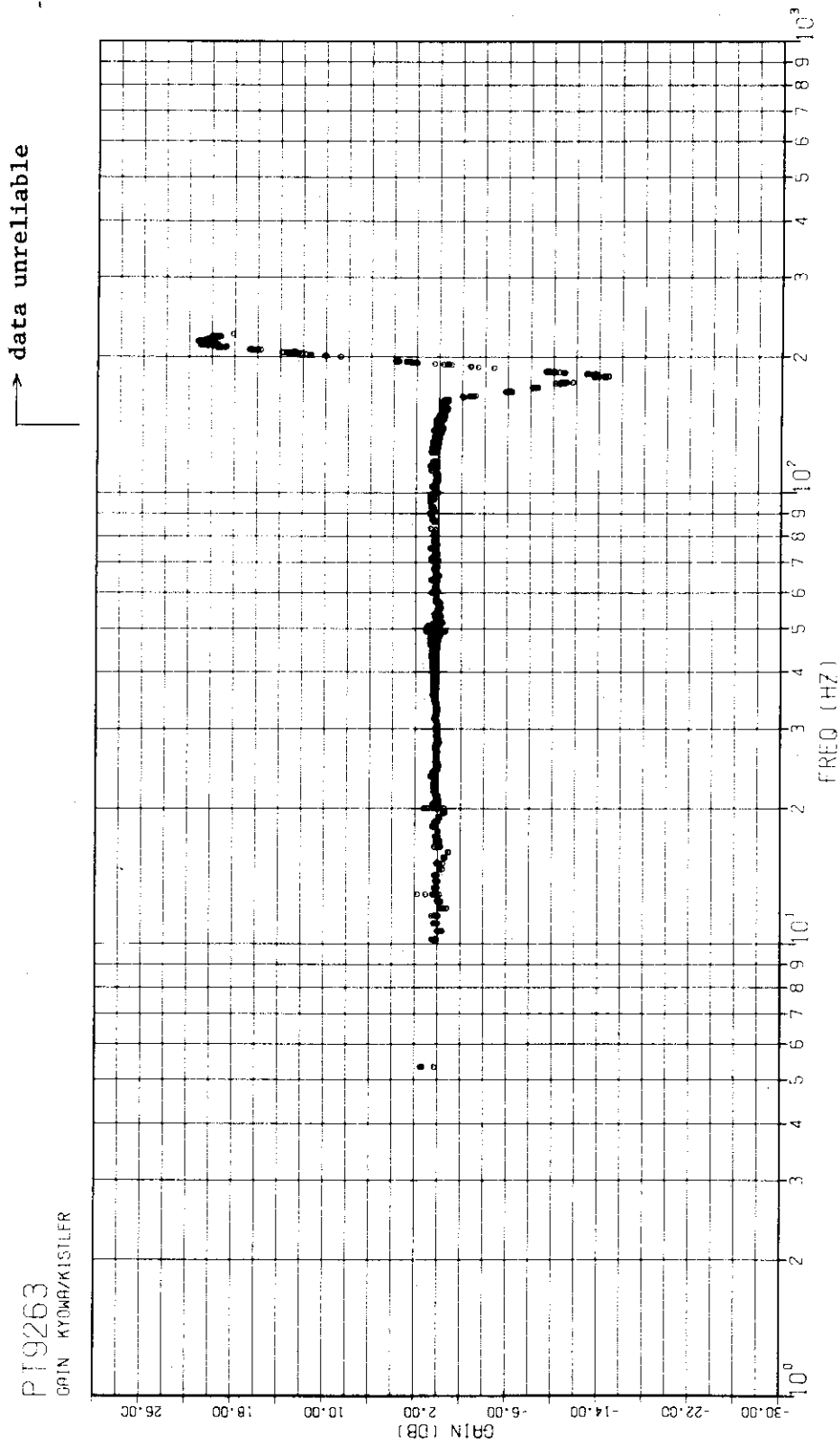


Fig. 30 Gain response of modified transducer, 150 kPa system pressure

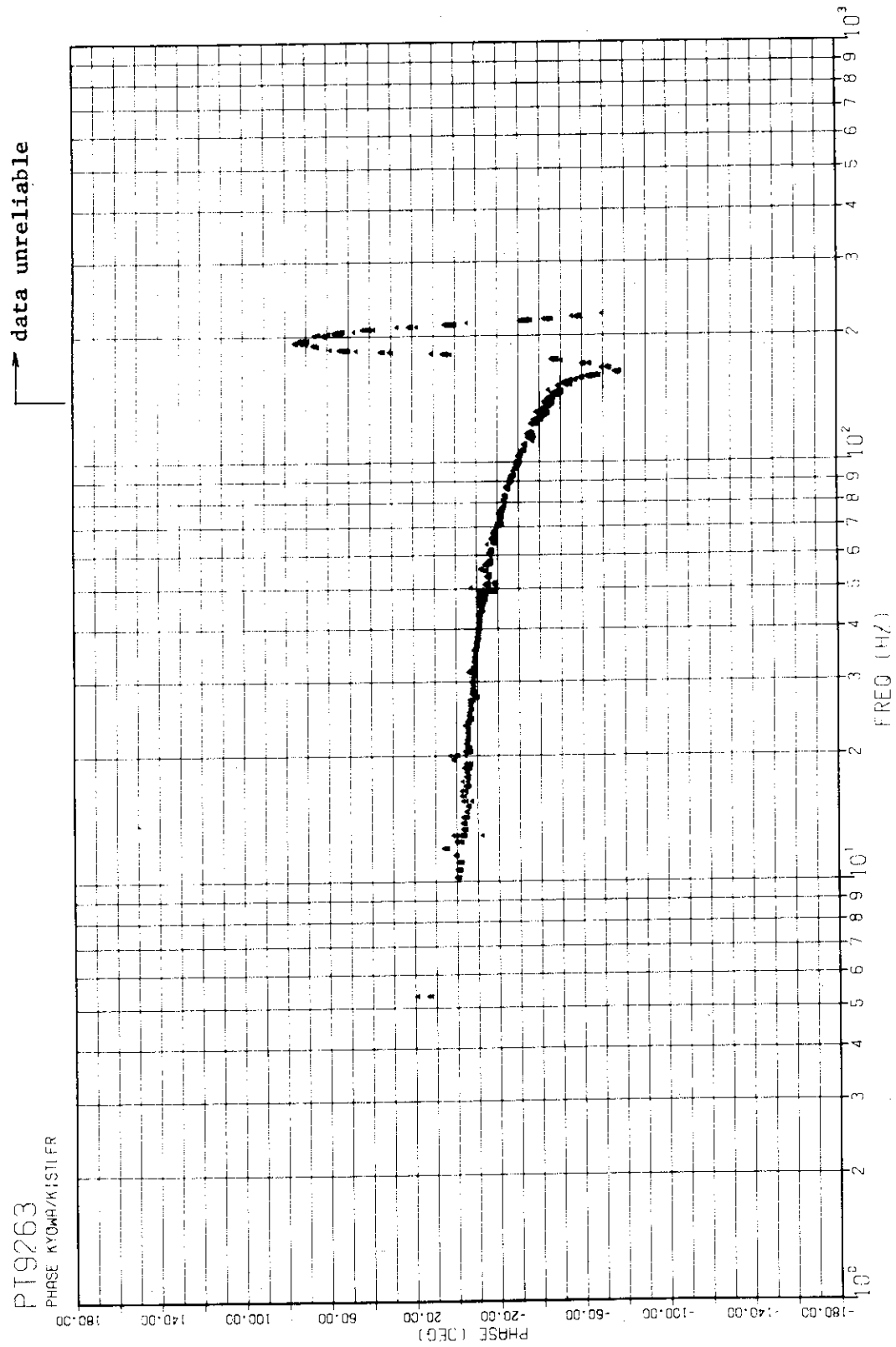


Fig. 31 Phase response of modified transducer, 150 kPa system pressure

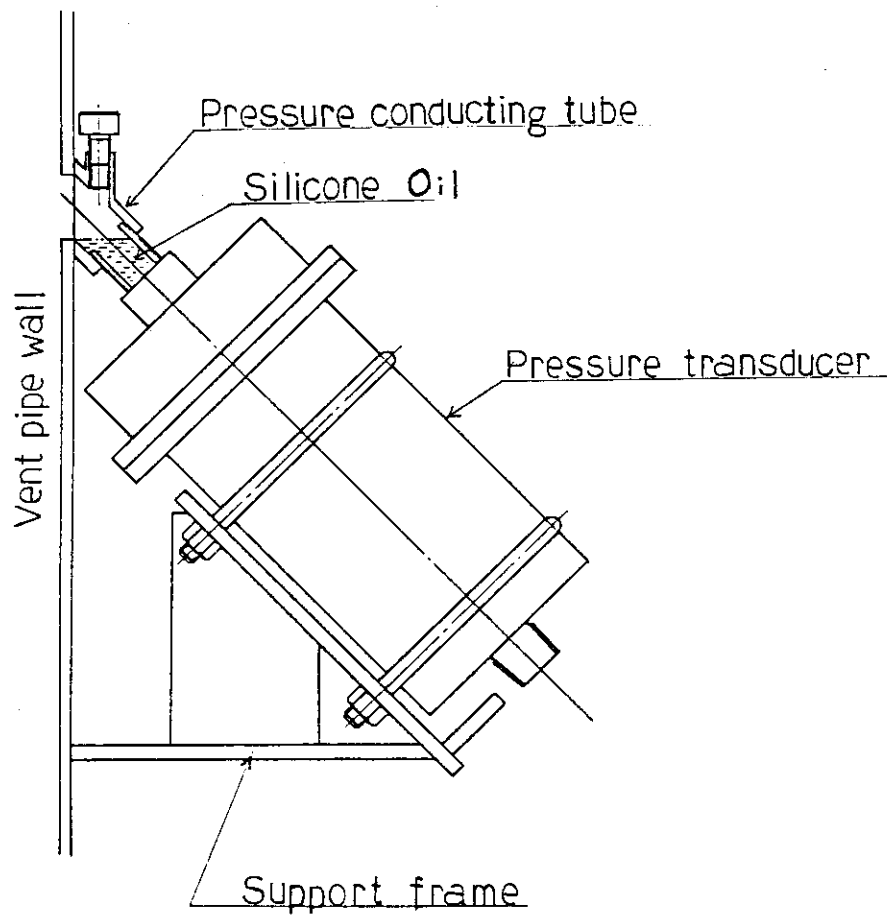


Fig. 32 Modified mounting scheme for vent pipe transducer

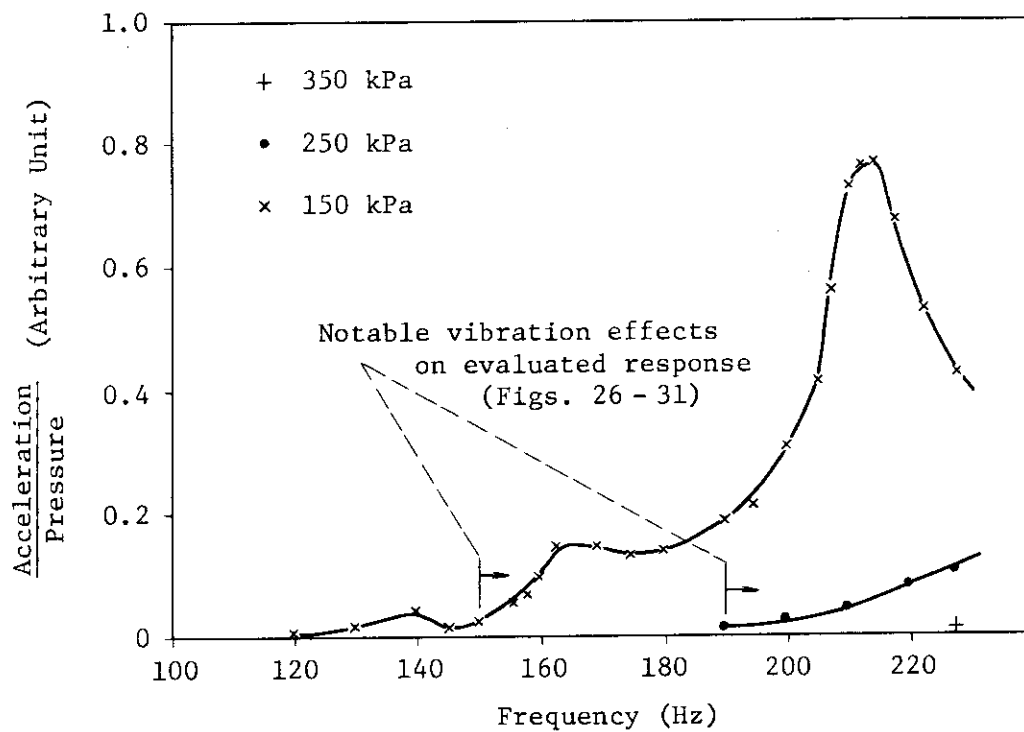


Fig. 33 Significance of system vibration effects during tests of modified transducer.

Appendix A Analysis of air bubble effects on transducer response

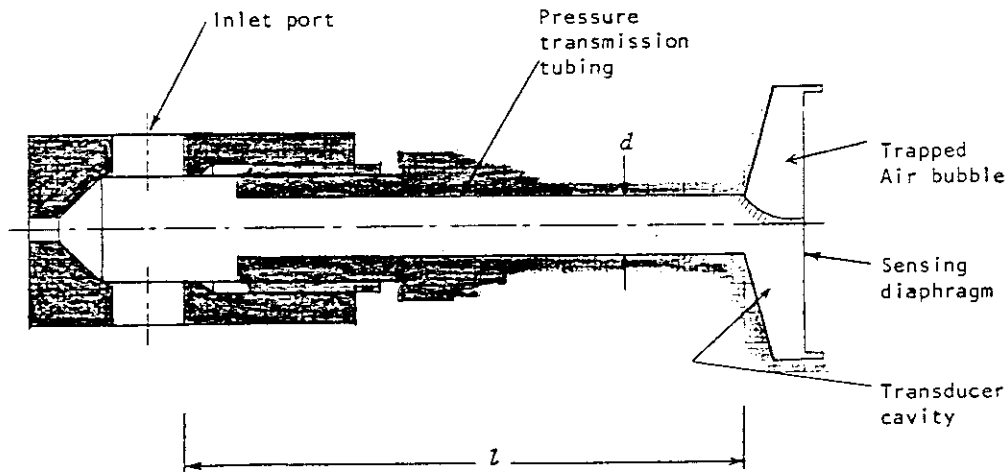
The dynamic response of a pressure transducer with pressure transmission tubing can be affected by presence of air bubbles in the tubing. Here, a simplified analysis is attempted on the air bubble effects on the response of the transducers formerly used for measurement of the pool bottom pressures in the CRT facility.

When air was present in the tubing the measured resonance frequencies were much lower than the acoustic natural frequency of the tubing filled with silicon oil (for sonic velocity c of 1400 m/s and tubing length L of 0.10 m, the fundamental natural frequency $f_0 = c/4L$ is about 3500 Hz), so the silicon oil can be approximated to be an incompressible fluid, or a rigid body. As shown in Figs. 16 through 21 the resonance frequency increased with the system pressure almost proportionally, which suggests that the pressure transmission line containing air bubbles can be approximated by a linear second-order system shown in Fig. A.1 where the spring compliance stems mainly from the air compressibility. A-1), A-2) As shown in the equations in Fig. A.1 the volumetric compressibility $\frac{\partial V}{\partial p}$ of air, whose volume changes adiabatically with rapid pressure variation and isothermally with quasi-static changes of the system pressure, is inversely proportional to the square of the system pressure. Therefore, if effective mass of the system does not change, the natural frequency is proportional to the system pressure.

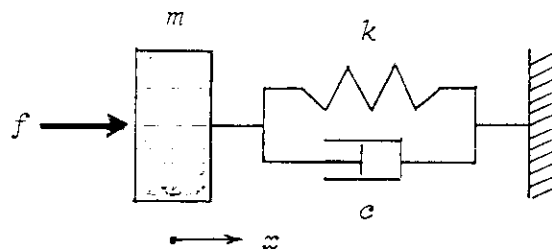
It might be assumed that the initial volume of air in the pressure transmission line of the horizontally mounted transducer is about one half of the transducer cavity volume. The effective mass of silicon oil may be approximated by ρlA . With these assumptions the natural frequencies of the transmission line were calculated and showed a close agreement with the test results as shown in Fig. A.2.

Reference for Appendix A

- A-1) R.C. Anderson and D.R. Englund, Jr., "Liquid Filled Transient Pressure Measuring Systems: A Method of Determining Frequency Response", NASA TN D-6603, Dec. 1971.
- A-2) T.B. Thomsen, "The Effect of Tubing on Dynamic Pressure Recording", NAA-TR-61-3, North American Aviation, Inc., Feb. 1961.



Schematic view of the pressure transmission tubing.



Simplified model for the above.

The liquid motion x is approximately calculated by the linear second-order equation:

$$m\ddot{x} + c\dot{x} + kx = f = pA$$

where

m = effective mass of liquid = ρlA

c = damping factor (unknown)

A = cross-sectional area of tube = $(\pi/4)d^2$

V = air bubble volume

With isentropic compressibility of air bubble

$$\partial V / \partial p = V / p\gamma$$

and static change of bubble volume

$$V = p_0 V_0 / p$$

the system compliance k is expressed as

$$k = \Delta f / \Delta x = A^2 / (\partial V / \partial p) = p^2 A \gamma / p_0 V_0$$

Therefore, the natural frequency of the system is

$$\omega_N = (k/m)^{1/2} \propto p$$

Fig. A-1 Modeling of pressure transmission tubing

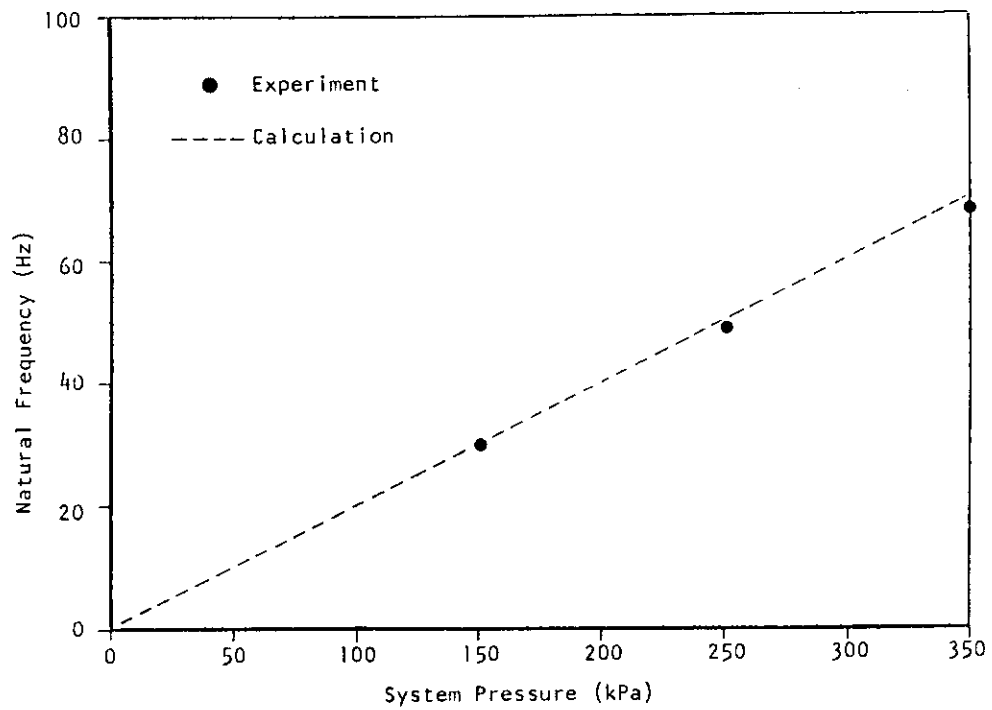


Fig. A-2 Comparison of measured and calculated natural frequencies of pressure transmission tubing containing air bubble

Appendix B Acceleration sensitivity of pressure transducer

During the dynamic pressure testing of the cavity-type transducer described in the main text, it was recognized that the transducer with a liquid-filled transmission line can be considerably sensitive to acceleration. The problem can be serious when small pressure changes are measured.

The present study of the acceleration sensitivity of the pressure transducer was motivated by the evaluation of test data obtained from TESTs 3103 to 3105 conducted from September to October 1981 after the modification of the pressure transducers. In these test runs a total of six flush-diaphragm transducers with semiconductor sensing element (Entran EPK-1251-300) were utilized together with the cavity-type transducers. The flush-diaphragm transducers formed pairs with six out of the seven cavity-type transducers on the pool bottom as shown in Fig. B.1.

A typical comparison of the output signals from the cavity-type and flush-diaphragm transducers is given in Fig. B.2. (The flush-diaphragm transducers exhibited fairly rapid thermal responses.) It was generally observed that the cavity-type transducer indicated higher peak amplitudes than the flush-diaphragm transducers. Since the flush-diaphragm transducer had a high resonant frequency of 120 kHz and was practically insensitive to acceleration, the plausible reason for the differences seemed to be transducer resonance at a frequencies higher than the tested range of 227 Hz, or effect of vibration of the transducer, or both. Since the built-in LPF of the pressure-transducer signal conditioner does not have a very efficient filtering characteristics above its nominal cut-off frequency of 250 Hz (Fig. 8), effect of aliased components could be considerable if the transducer exhibits significant resonances to pressure or acceleration above the Nyquist frequency of the data acquisition system (227 Hz for TESTs 3103 to 3105).

An acceleration sensitivity test of the transducer was conducted by using an electromagnetic shaker with a capacity of 100 G's for a frequency range of 10 to 1000 Hz. The test block diagram is illustrated in Fig. B.3. A cavity-type pressure transducer of the same design as used from TEST 3103 was mounted vertically on the shaker table. The test was conducted under the atmospheric pressure and for the axial acceleration alone. The output signal from the transducer and a accelerometer

mounted on the jig surface were recorded by an analog recorder. The built-in LPF of the transducer signal conditioner was not used. The recorded signals were processed by the same computer program as used in the dynamic pressure testing to evaluate the gain and phase responses of the transducer relative to acceleration.

Fig. B.4 shows results of a test where the pressure transmission tubing and the transducer cavity were not filled with silicon oil. Even without silicon oil the transducer exhibited a sensitivity to acceleration, because the transducer sensing diaphragm has a mass. The sensitivity increased with frequency. The discrepancies from the linear trends are due to resonances of the mounting jig which was not sufficiently rigid for the present tests.

Fig. B.5 shows results of a test with silicon oil filled up to the inlet ports of the tubing. The sensitivity increased to about eight times as large as that without silicon oil. Again, the jig vibration caused some errors of the evaluated transducer responses. For example, the discontinuous changes at about 300 Hz and 450 Hz correspond to the jig resonances. However, the tendency of the transducer response is fairly clear, and a resonance of the transducer at about 400 Hz can be identified.

This resonance frequency is several times higher than that of the transducer with air bubbles in the tubing, which was studied in Appendix A, however, still much lower than the acoustic natural frequency of the tubing. Therefore, the pressure transducer with a completely silicon-filled tubing can be again approximated by a linear second-order system shown in Fig. B.6. This time compliance mainly comes from that of the transducer sensing diaphragm, and the external force does not act on the mass (of silicon oil) directly. However, as shown in Fig. B.6, the equation of motion for this case can be easily reduced into the same form as for the case when the external force acts directly on the mass (cf. Fig. A.1). It has an interesting implication that an acceleration sensitivity test is equivalent to a dynamic pressure response test. As stated in the main text of this report, the dynamic pressure test was not successful beyond about 200 Hz because of significant vibration of the test apparatus. The present results of the acceleration test indicates that the transducer will be resonant to pressure or acceleration inputs at around 400 Hz. The transducer gain at the resonance frequency will be about three times greater (+10 dB) than that at the frequencies below 160 Hz.

The LPF loss at 400 Hz is about 8 dB and may not be enough to

eliminate the effect of the transducer resonance on the signal aliasation: with the present Nyquist frequency of 227 Hz, the signal component at around 400 Hz will be aliased at around 150 Hz. However, since of interest is the signal components below 100 Hz, and mostly below 50 Hz, when we are to evaluate the containment hydrodynamic loads due to the pressure oscillation, the high-frequency characteristics studied in this Appendix will not have a significant influence on the evaluated magnitudes of the containment loads.

The natural frequency was calculated with the model shown in Fig. B.6 using a value of the diaphragm compliance shown in the figure reported by the vendor. The calculated natural frequency was 450 Hz which is about 10% higher than the measured natural frequency.

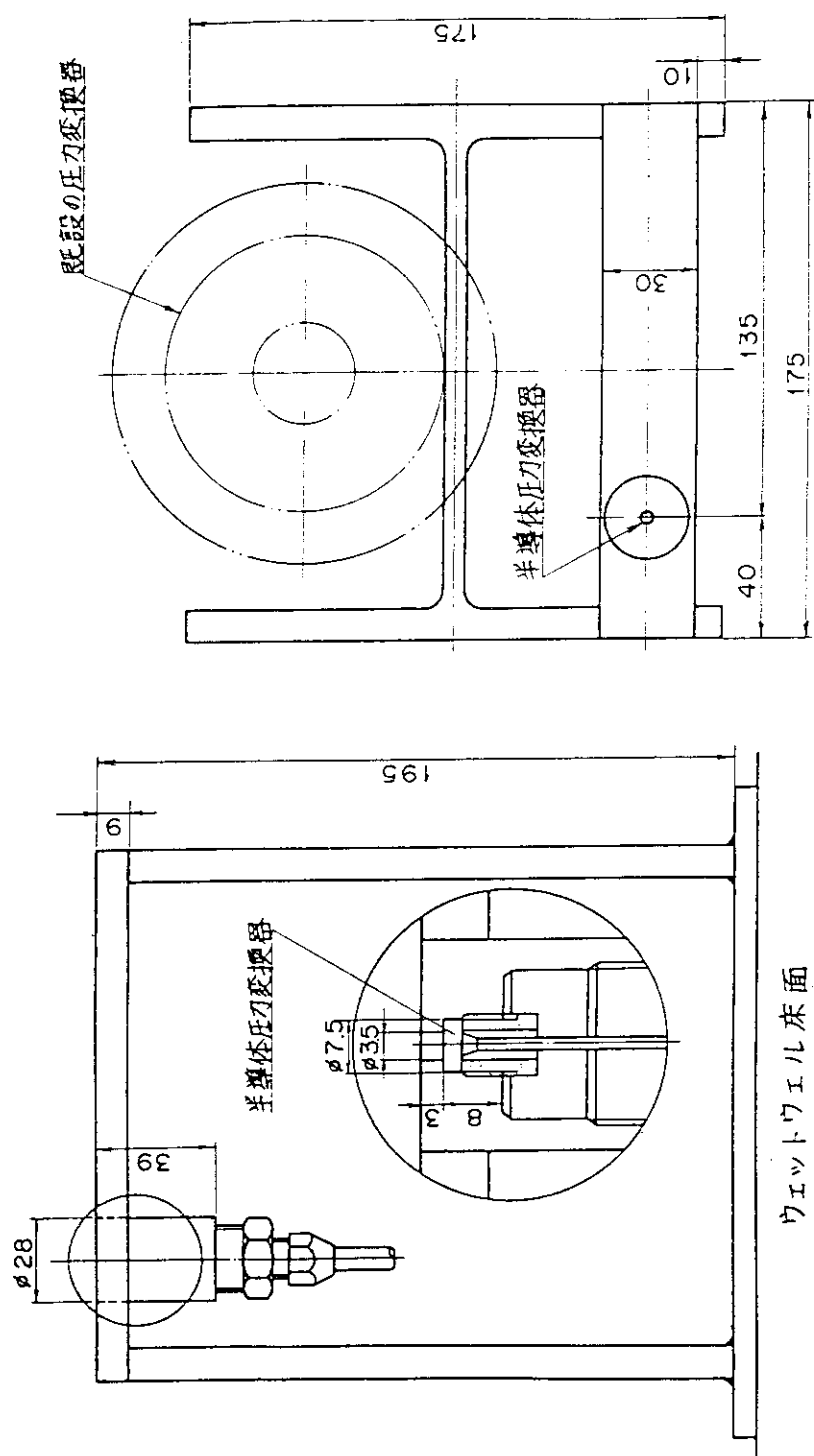


Fig. B-1 Mounting scheme of Entran flush-diaphragm pressure transducer

FULL-SCALE MARK II CRT

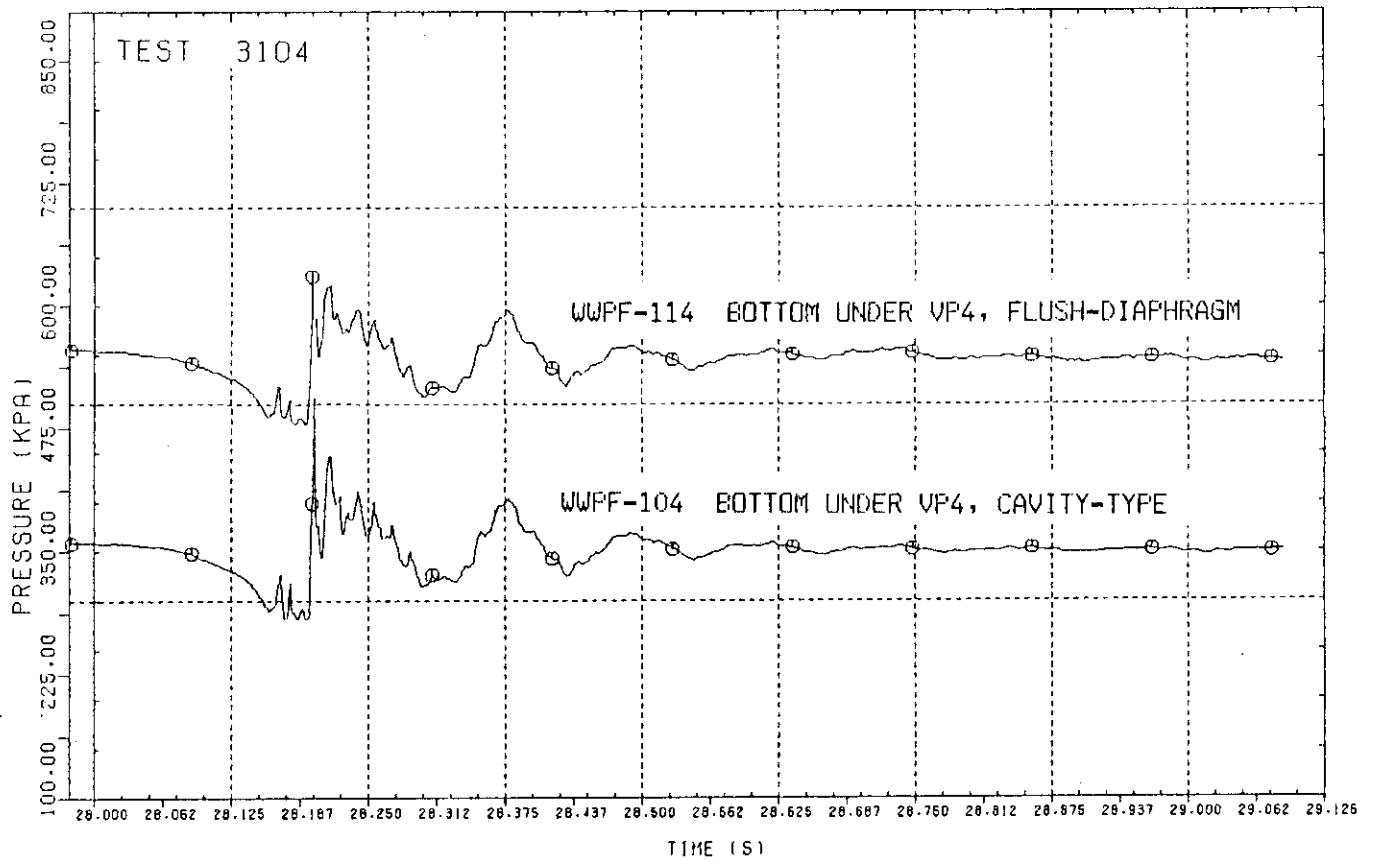


Fig. B-2 Comparison of output signals from flush-diaphragm and cavity-type pressure transducers

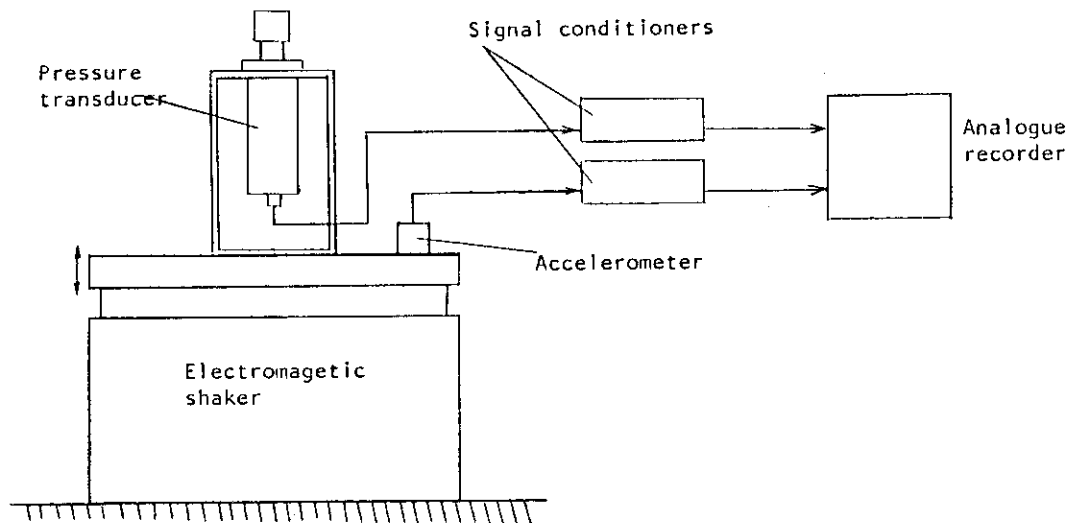


Fig. B-3 Setup of acceleration sensitivity test

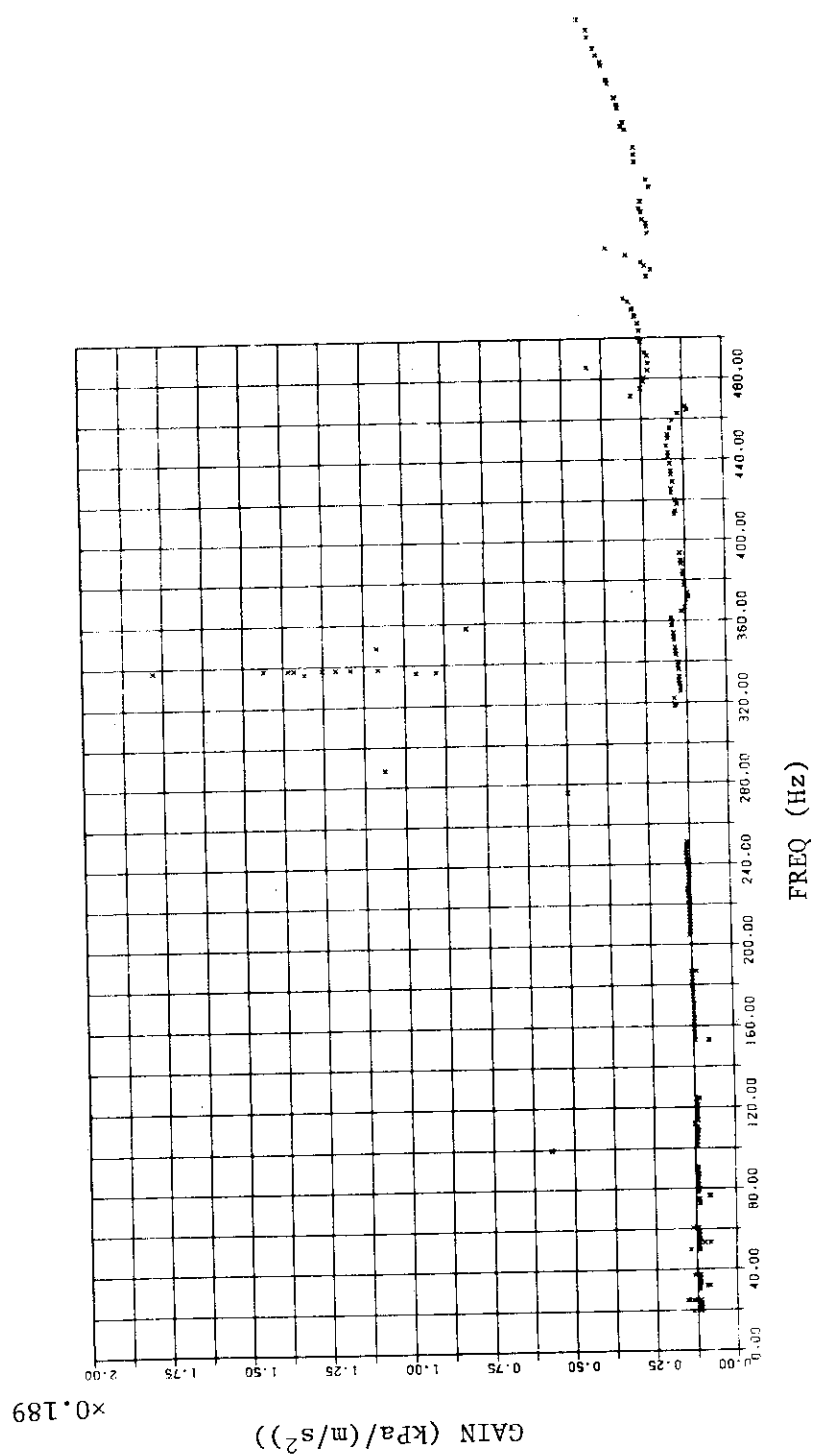


Fig. B-4 Acceleration sensitivity of pressure transducer without silicon oil

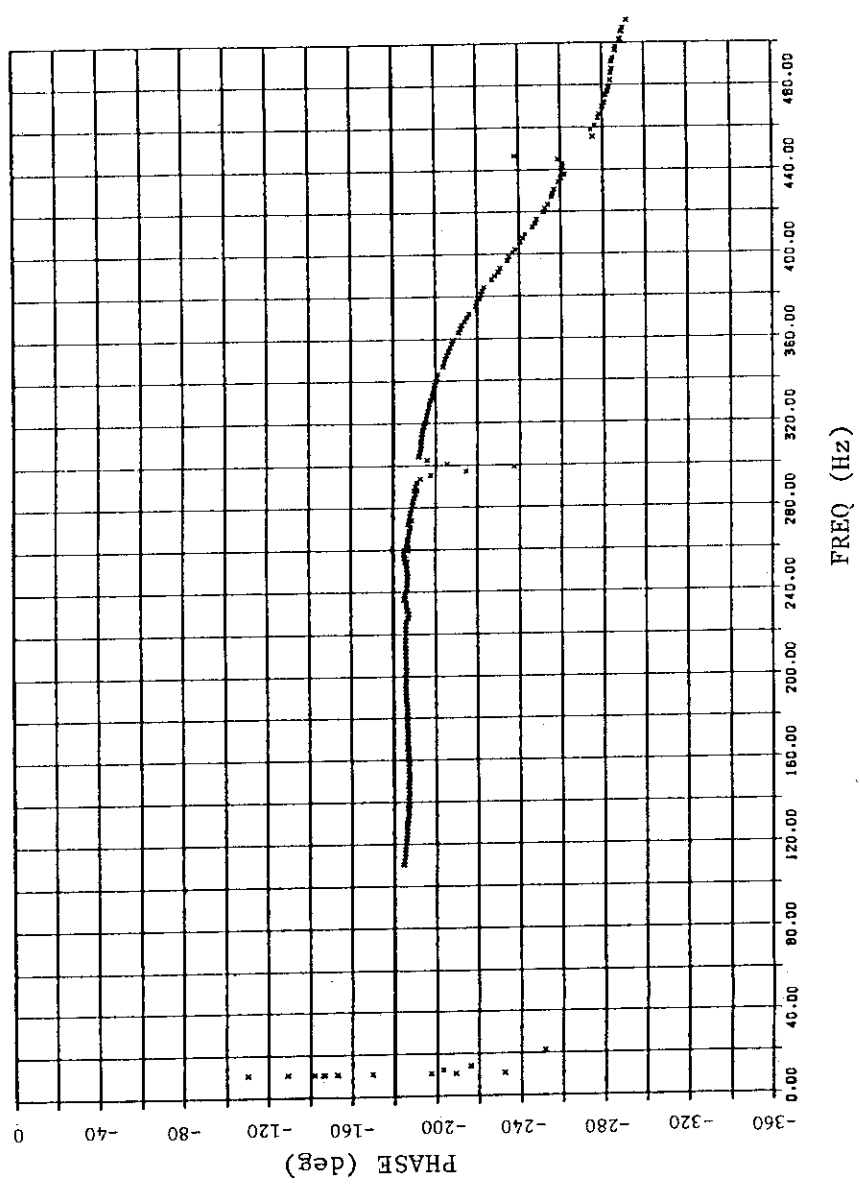
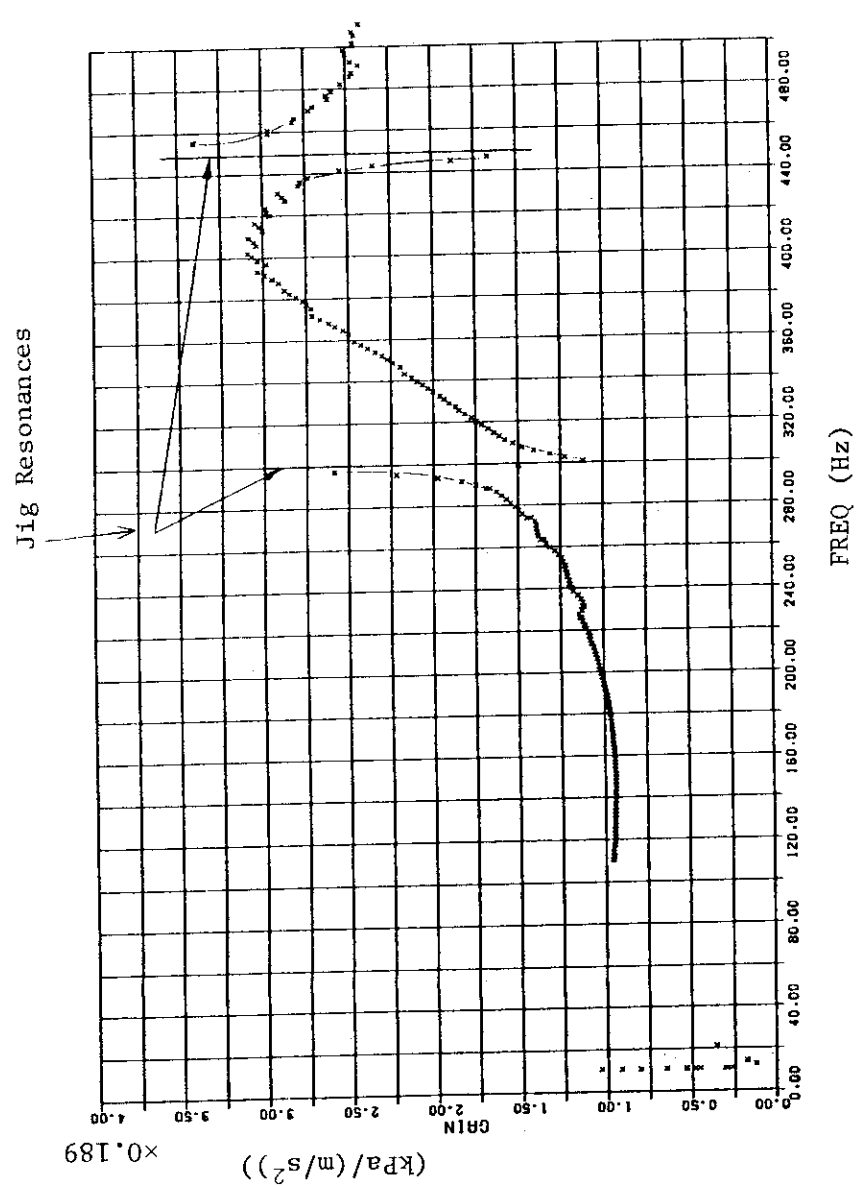
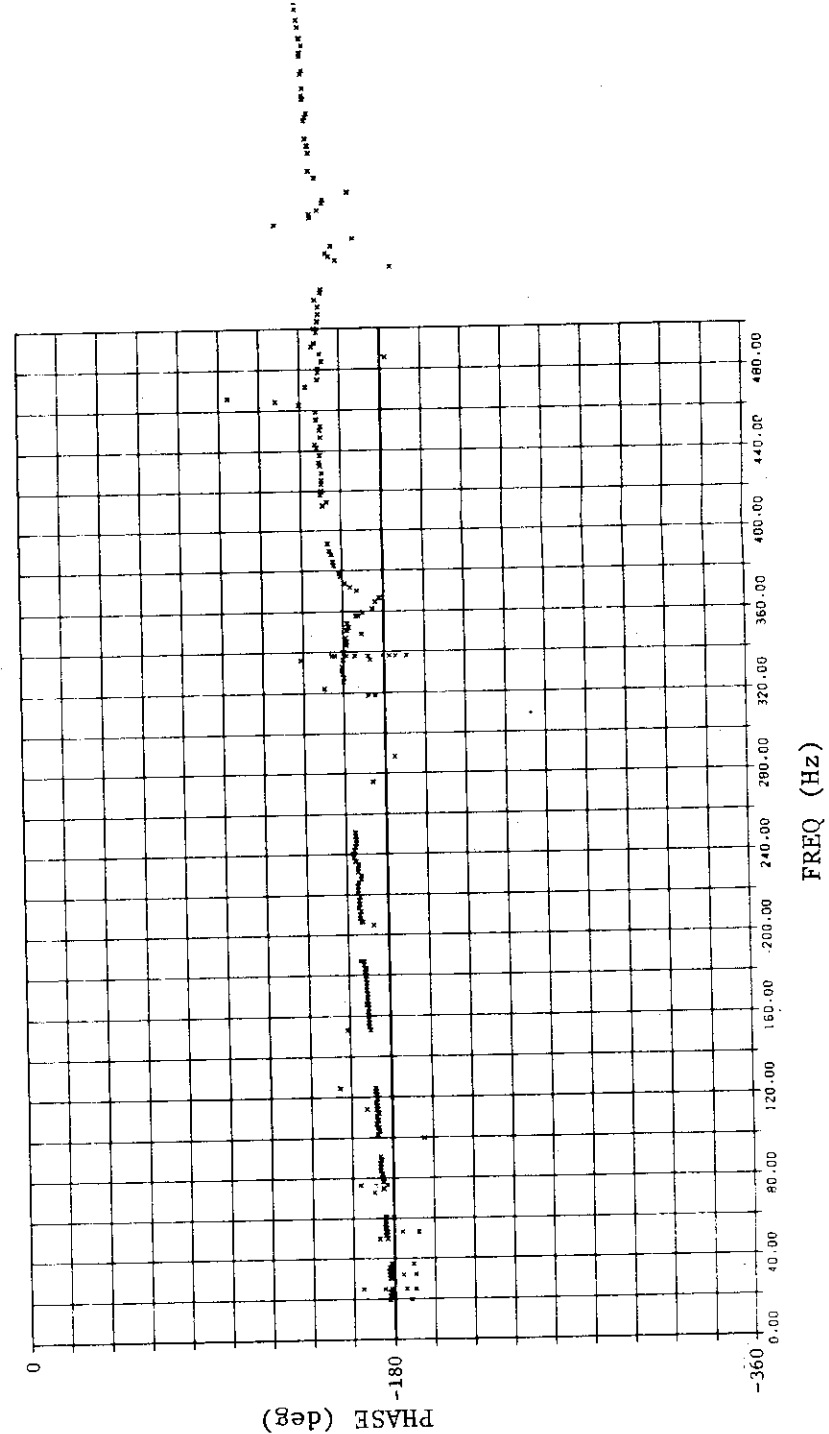
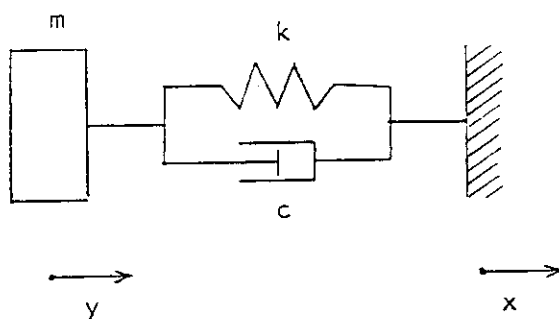


Fig. B-5 Acceleration sensitivity of pressure transducer with silicon oil filled in pressure transmission line

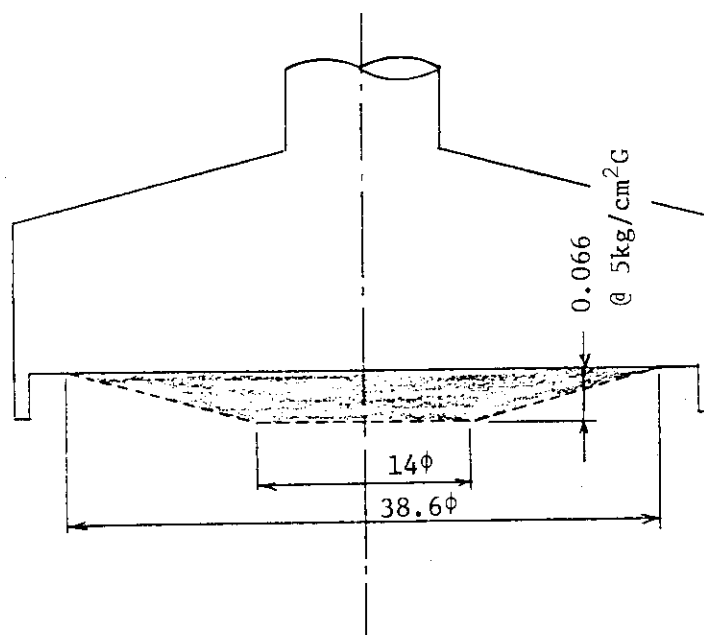


The liquid column motion y due to the transducer forced motion x is approximately expressed as:

$$m\ddot{y} = -k(y-x) - c(\dot{y}-\dot{x})$$

Introducing $z = (y-x)$ we get

$$m\ddot{z} + c\dot{z} + kz = -m\ddot{x}$$



Deformation of transducer cavity

Fig. B-6 Modeling of transducer response to acceleration

Appendix C Further improvements on pressure measurement

In parallel with conducting the dynamic response evaluation test and modifications of the cavity-type transducers described in the main text, additional measurement was made in the blowdown tests with transducers which have good and known dynamic response characteristics.^{C-1)} Two different types of flush-diaphragm transducers were used. From TEST 3103 through TEST 3105 six Entran EPK-125-300 semiconductor-type transducers were used for the pool bottom measurement. From TEST 3106 till the end of the test program a total of twenty-six (26) Senso-Metrics Model 601087 strain-gage type transducers were used for the pool and vent pressure measurements. Both types of the transducers are designed to have high (>10 kHz) resonance frequencies and installed with no pressure tubing, but their sensing diaphragms were coated with RTV (room temperature vulcanizing) material which have very small thermal conductivity to reduce the temperature effects on the pressure measurements. The RTV-coated Senso-Metrics transducers were tested by the Lawrence Livermore National Laboratory and proved to have still very high resonance frequencies in spite of the addition of mass on the sensing diaphragm.^{C-2)}

Many of the new transducers were installed in the facility so that they form pairs with adjacent cavity-type transducers in order to monitor the dynamic response of the cavity-type transducers during the blowdown tests through comparison of the output signals. Cross-spectral quantities were calculated using an FFT computer program developed for the analysis of the blowdown test data.^{C-3)} Time periods were chosen from the test data where magnitudes of the high frequency components of the pressure oscillation were sufficiently large to obtain appropriate S/N ratios.

Figs. C-1 and C-2 show typical results of evaluation. In these figures a positive phase angle indicates a positive phase lag. A high coherency between the signals implies a high S/N ratio and therefore a meaningful evaluation. Accordingly, the present evaluation may be valid up to 160 Hz. The results of this evaluation once again confirm that the dynamic response of the cavity-type transducer was adequate for this frequency range.

References for Appendix C

- C-1) Yamamoto, N., "Full-Scale Mark II CRT Program: Improvements on Test Measurements," JAERI-M report to be published.
- C-2) Altes, R.G. et al., "Mark I 1/5-scale Boiling Water Reactor Pressure Suppression Experiment Facility Report," UCRL-52340, Oct. 1977
- C-3) Kukita, Y. et al., "Statistical Evaluation of Steam Condensation loads in Pressure Suppression Pool," JAERI-M 9665, Oct. 1981

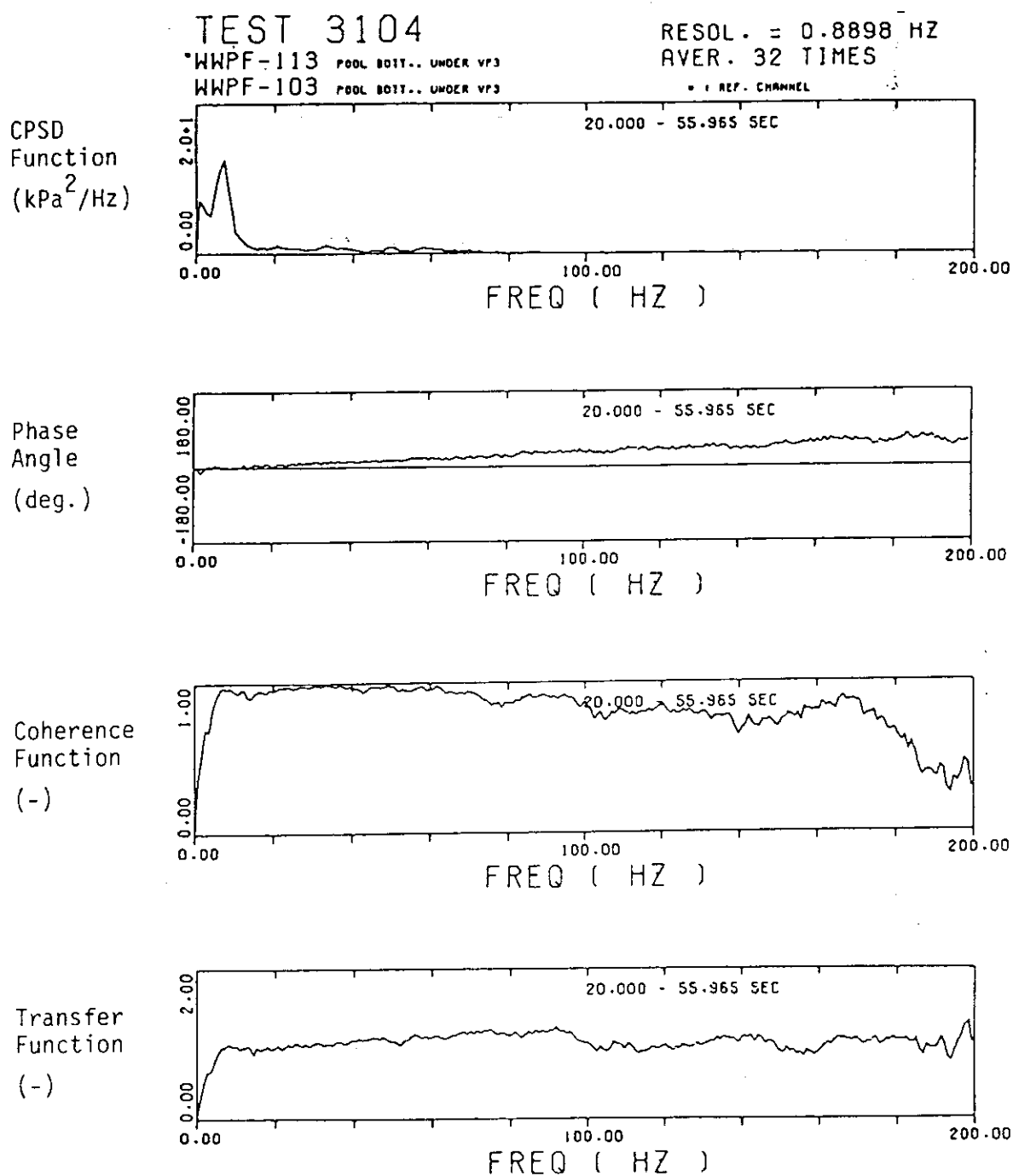


Fig. C-1 Dynamic response of cavity-type transducer evaluated using Entran transducer as reference

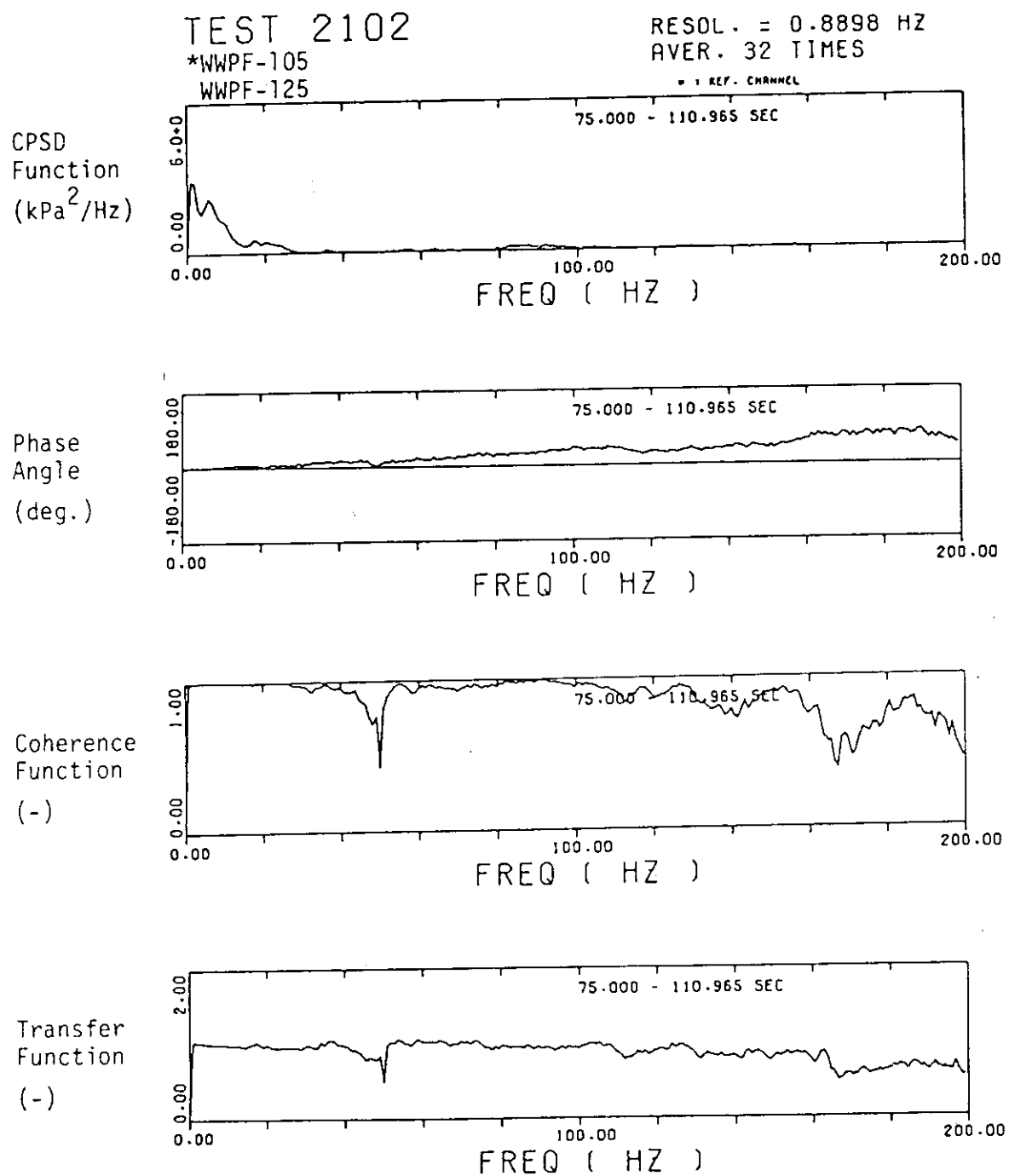


Fig. C-2 Dynamic response of cavity-type transducer evaluated using Senso-Metrics transducer as reference